โครงการการเรียนการสอนเพื่อเสริมประสบการณ์

ลักษณะเฉพาะทางคลื่นไหวสะเทือนของหินอัคนีแทรกซอน
ในแอ่งแคนเทอร์เบอรี ประเทศนิวซีแลนด์

โดย

นายชวัลวิทย์ หลีอาภรณ์
เลขประจำตัวนิสิต 5732712523

โครงการนี้เป็นส่วนหนึ่งของการศึกษาระดับปริญญาตรี
ภาควิชาธรณีวิทยา คณะวิทยาศาสตร์ จุฬาลงกรณ์มหาวิทยาลัย
ปีการศึกษา 2560

SEISMIC CHARATERISTICS OF IGNEOUS INTRUSIONS

IN CANTERBURY BASIN, NEW ZEALAND

Mr. Chawanwit Lee-arporn

A Project Submitted in Partial Fulfillment of the Requirements

For the Degree of Bachelor of Science Program in Geology

Department of Geology, Faculty of Science, Chulalongkorn University

Academic Year 2017

ลักษณะเฉพาะทางคลื่นไหวสะเทือนของหินอัคนีแทรกซอน

ในแอ่งแคนเทอร์เบอรี่ ประเทศนิวซีแลนด์

นาย ชวัลวิทย์ หลือาภรณ์

Project Title   SEISMIC CHARATERISTICS OF IGNEOUS INTRUSIONS

IN CANTERBURY BASIN, NEW ZEALAND

By   Mr. Chawanwit Lee-arporn

Field of Study   Geology

Project Advisor   Piyaphong Chenrai, Ph.D.

_____

Submitted date……………………………………….

Approval date……………………………………….

……………………………………………………….

Project Advisor

(Piyaphong Chenrai, Ph.D.)

ชวัลวิทย์ หลีอาภรณ์ : ลักษณะเฉพาะทางคลื่นไหวสะเทือนของหินอัคนีแทรกซอน ในแอ่งแคนเทอร์เบอรี่ ประเทศนิวซีแลนด์. (SEISMIC CHARATERISTICS OF IGNEOUS INTRUSIONS IN CANTERBURY BASIN, NEW ZEALAND) อ.ที่ปรึกษาโครงงาน : อาจารย์ ดร. ปิยพงษ์ เชนร้าย, 57 หน้า.

การปะทุของภูเขาไฟในประเทศนิวซีแลนด์เริ่มต้นขึ้นในช่วงปลายยุคครีเทเชียสถึงสมัยไพลโอซีน อย่างไม่ต่อเนื่องในหลายช่วงเวลา และเกิดขึ้นอย่างกระจัดกระจายในพื้นที่ ทำให้เกิดหินอัคนีแทรกซอนขึ้นในแอ่งแคนเทอร์เบอร์รี่ ซึ่งเป็นแอ่งหนึ่งที่มีศักยภาพเชิงปิโตรเลียมในประเทศนิวซีแลนด์ ในงานศึกษานี้ ข้อมูลคลื่นไหวสะเทือนแบบ 3 มิติ ของพื้นที่ศึกษา ถูกใช้เพื่อแปลความหมายคลื่นไหวสะเทือนที่แสดงถึงหินอัคนีแทรกซอน โดยพบหินอัคนีแทรกซอนทั้งหมด 5 หน่วย มีรูปร่างทั้งหมด 3 แบบ ประกอบด้วยรูปถ้วย (Saucer shaped sill), รูปแผ่นเอียง (Inclined sheet) และ รูปแผ่นราบ (Layer-parallel sheet) เมื่อใช้รูปร่างและตำแหน่งการวางตัวของหินอัคนีแทรกซอนจะทำให้สามารถทำนายทิศทางการไหลของหินหนืดและบริเวณแหล่งต้นกำเนิดของหินอัคนีแทรกซอนที่มีรูปร่างแตกต่างกันไปได้ นอกจากนี้การวิเคราะห์รูปร่างหินอัคนีแทรกซอนและลักษณะเชิงคลื่นไหวสะเทือนของหินปิดทับบ่งชี้ว่าหินอัคนีแทรกซอนรูปถ้วย (Saucer shaped sill) มีผลให้เกิดโครงสร้างคล้ายโดมที่เรียกว่าการคดโค้งจากการแทรกดัน (Forced fold) ซึ่งอาจจะเป็นโครงสร้างกักเก็บปิโตรเลียมได้ ข้อมูลคลื่นไหวสะเทือนแบบ 2 มิติ และข้อมูลหลุมเจาะที่ใช้ในการเทียบสัมพัทธ์ลำดับชั้นหินร่วมกับการวิเคราะห์ลำดับชั้นหินเชิงคลื่นไหวสะเทือนชี้ให้เห็นว่าช่วงเวลาของการแทรกดันของหินอัคนีแทรกซอนเกิดขึ้นตั้งแต่สมัยไมโอซีนซึ่งเป็นช่วงเวลาใกล้เคียงและคาบเกี่ยวกันกับช่วงเวลาการกำเนิดปิโตรเลียมในแอ่ง ดังนั้นแล้วโครงสร้างการคดโค้งเนื่องการการแทรกดัน (Forced fold) ที่เป็นผลจากการแทรกดันของหินอัคนีแทรกซอนรูปถ้วยอาจมีศักยภาพในการเป็นโครงสร้างกักเก็บปิโตรเลียมได้

ภาควิชา .... ธณีวิทยา .... ลายมือชื่อนิสิต ....
สาขาวิชา .... ธรณีวิทยา .... ลายมือชื่อ อ.ที่ปรึกษา ....
ปีการศึกษา .... 2560 ....

5732712523: MAJOR GEOLOGY

KEYWORDS: IGNEOUS INTRUSIONS / CANTERBURY BASIN / SEISMIC CHARATERISTICS / SAUCER SHAPED / FORCED FOLD

CHAWANWIT LEE-ARPORN: SEISMIC CHARATERISTICS OF IGNEOUS INTRUSIONS IN CANTERBURY BASIN, NEW ZEALAND. ADVISOR: PIYAPHONG CHENRAI, Ph.D., 57 pp.

In New Zealand, the volcanism commenced in the Late Cretaceous to Pliocene intermittently and locally and caused igneous intrusions in the Canterbury basin, one of the petroliferous frontier basins in New Zealand. In this study, 3D seismic data of WAKA 3D were used to interpret seismic reflectors of igneous intrusions. Five sills units and three morphologies of sills were discovered including; a saucer shaped sill, an inclined sheet and a layer-parallel sheet. Using sill geometries and sill stratigraphic positions, the inferred magma flow direction and potential sources were derived for each sill unit. Plus, an analysis of sill geometry and seismic characteristics of overburden rocks proposes saucer shaped sill induced the dome like structure called forced fold above which could be a trap for petroleum systems. Additionally, 2D seismic data and well data used to make correlation integrated with the seismic-stratigraphic analysis imply that emplacement timing of sills has started since Miocene which overlapped to the time of hydrocarbon generation. Consequently, forced folds induced by saucer shaped sill can possibly be a potential trap.

Department: _____Geology_____ Student's Signature_____

Field of Study: _____Geology_____ Advisor's Signature_____

Academic Year: _____2017_____

Acknowledgement

I gratefully acknowledge my advisor, Piyaphong Chenrai, Ph.D., for great support and suggestions throughout work processes. I really appreciate my advisor for pushing me to unleash my potential as much as possible and thank for his respect to any actions I took and ideas I had. This report could not have been done without his invaluable advice.

I also thank all the associates of geology department for supporting me when I had been studying in this department.

Besides, I would like to thank our project team including Mr. Natcharphol Chansiri, Mrs. Boontigan Koohasuppasin, Mrs. Tanita Chaiyasit for any advice and suggestions during working on this project.

Finally, I would like to give the special thanks to my family who has been supporting me and respecting to my thoughts and any decisions I have made so far.

Table of contents

List of tables

List of figures

Chapter1

Introduction

1.1   Background and significance

The Canterbury basin has a well-defined petroleum system, with mature source, reservoir, seal rocks and traps (Sahoo et al., 2015). Besides there are igneous intrusions, found in the basin (Sahoo et al., 2015), which are important to be studied in details before conducting further hydrocarbon exploration and production. Igneous intrusions could make the geology of the field areas change in several ways; for example, they induce domal uplift (forced fold) which could be a trap or petroleum accumulation(Kumar et al., 2013, Holford et al., 2012). Furthermore, fractures in some rocks could be enhanced and turned to be potential reservoirs. Additionally, the thermal effect of igneous intrusion sometimes has favorable influence on hydrocarbon generation, accelerating the maturation of hydrocarbon (Galushkin, 1997; Fjeldskaar et al., 2008). However, igneous intrusions can cause problems sometimes during phases of drilling; such as a slow drilling speed (Millett et al., 2016). Accordingly, it is so essential to study igneous intrusions in the sedimentary basin that has petroleum potential for the highest benefits of hydrocarbon exploration and production.

Besides, igneous intrusions do not expose all their bodies on the surface and mostly they intrude sedimentary rocks within subsurface, so using seismic reflection data which allow us to study subsurface geology is one of the best ways to apply for this study. The study of igneous intrusions from seismic data can provide benefits for the understanding of seismic geometry, distribution and characteristics of igneous intrusions comprehensively. The seismic interpretation will allow us to detect the position and distribution of igneous bodies. Besides, the mechanism of magma flow patterns or igneous intrusion emplacements will be examined with help of detailed interpretation of their true geometries (Thomson and Hutton, 2004). The results of this study could lead us to understand the processes of volcanism in the study area which might be linked to tectonic setting in the Canterbury basin.

1.2   Objective

To analyze the seismic characteristics, geometries and distribution of igneous intrusions.

1.3   Study area

The study area is in WAKA 3D block (3D seismic volume), having length of 72 kilometers and width of 20 kilometers and covering 1,440 km^2 (Fig. 1.1) It is located at the grid position at latitude of 183.12 degrees decimal and longitude of -45.35 degrees decimal in the 59G zone of southern hemisphere. The study area is in the Canterbury basin located on the east coast of the southern island of New Zealand.
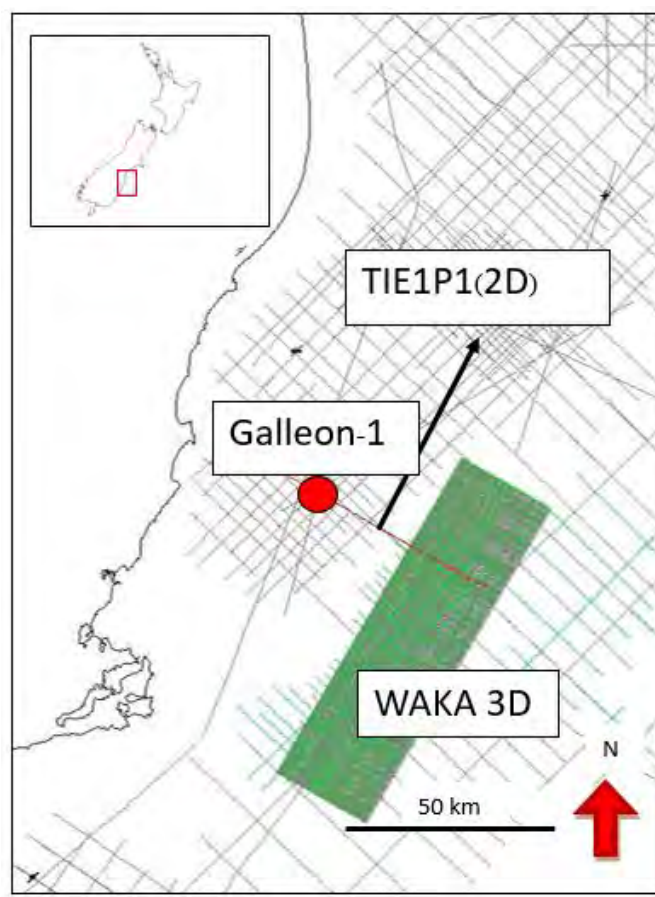
Fig. 1.1. The study area, Waka-3D block in the Canterbury basin, New Zealand.

1.4 Methodology

The study of seismic igneous intrusions can be divided into 3 main phases below

a. Interpret 3D seismic reflection data of WAKA 3D to identify all possible igneous intrusions of the Canterbury basin and visualize them with amplitude extraction and opacity rendering methods to see the geometries, characteristics, distribution and locations of them. The result will be the map of locations and distribution of seismic igneous intrusions and the descriptions of the seismic characteristics of each igneous intrusion identified.

b. Perform well data correlation from the nearest well (Galleon-1) from WAKA 3D with 2D line passing through both the well of Galleon-1 and WAKA 3D and correlate the relative age of horizons of rock formations from tangible data (well data) to intangible data (3D seismic reflection data).

c. Analyze the results of interpretation and make assumptions of potential magma feeders, flow patterns and emplacement ages of igneous intrusions correlated to host rocks and conclude.

The workflow and expected results are shown below (Fig.1.2).

WORKFLOW

- Interpret seismic data to identify all possible igneous intrusion and visualize them.

- Perform well data for correlation between tangible data and intangible data.

- Analyze the results of interpretation

EXPECTED RESULTS

- The map of igneous intrusions in the study area
- Locations, distribution and geometries of igneous intrusions

- Ages of horizons and host rocks bearing igneous intrusions

- Potential magma feeder zones
- Flow pattern and emplacement timing of igneous intrusions

Fig. 1.2. The workflow and expected results of the study.

Chapter 2

The Geology of the study area

2.1 The general information of the Canterbury basin

The Canterbury Basin contains up to 6 km of strata, thickest in the Clipper Sub-basin which one of many sub-basins (Fig. 2.3) and covers more than 40,000 square kilometers in both onshore and offshore. It extends east into deeper water of the Bounty Trough and is contiguous south with the much larger Great South basin (Fig. 2.1).
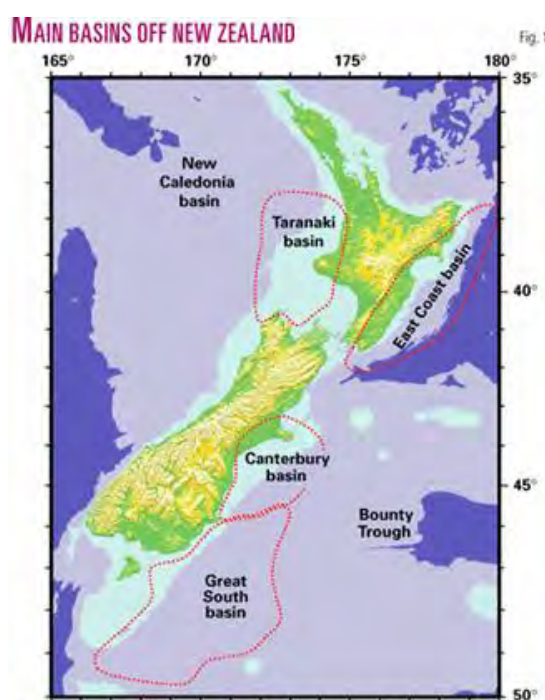
Fig.2.1. The Canterbury basin in New Zealand (Sutherland and Browne, 2003).

Additionally, it is one of the petroliferous frontier basins in New Zealand and is under active exploration in multiple permits. Sub-commercial gas and condensate discoveries suggest that it has a working petroleum system. Accordingly, this basin is interesting for further studying in the aspect of petroleum exploration and production.

2.2   The tectonic settings and chronostratigraphy of the Canterbury basin

The general geology, basin evolution, and paleogeographic development since the Cretaceous have been described by several authors (e.g. Field and Browne, 1989; Constable and Crookbain, 2011). The Canterbury basin is an intra-continental rift and subsequent sag basin (Sahoo et al., 2015). The tectonic evolution of the Canterbury basin can be divided into four main phases (Sutherland and Browne, 2003).

1) Permian to Jurassic convergent margin.
2) mid-Cretaceous rifting.
3) Late Cretaceous to Oligocene passive subsidence.
4) Miocene to Recent transcurrent tectonics.

The 4 phases of tectonic evolution are shown below (Fig. 2.2).
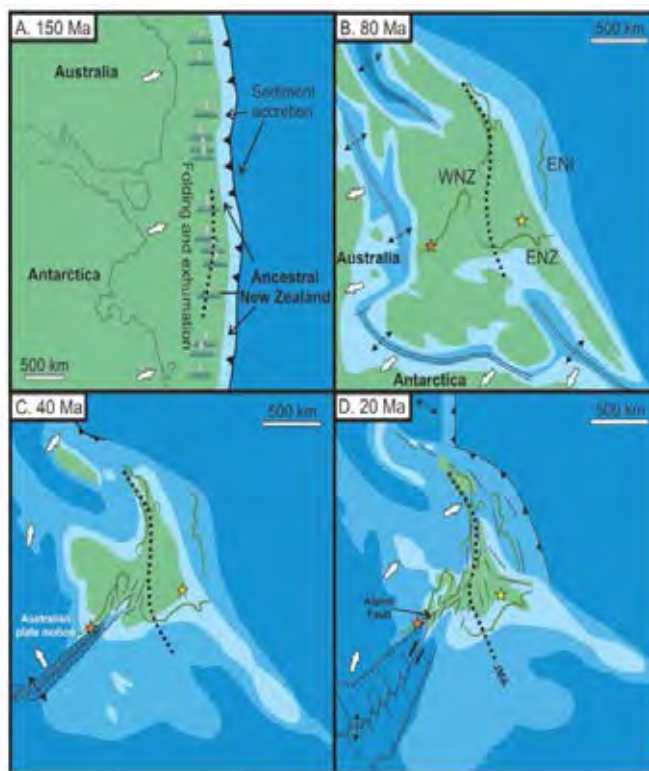
Fig. 2.2. Four main phases of tectonic evolution of the Canterbury basin
(Cox and Sutherland, 2007).

First, a large number of clastic sediments were deposited and complexly folded in an accretionary convergent margin in Permian to Jurassic. Most of these rocks are considered economic basement below which rock layers are not expected to contain commercial hydrocarbons (Sutherland and Browne, 2003).

Secondly, mid Cretaceous, it began life as an extensional fault-angle basin due to the crustal stretching that accompanied the beginnings of opening of the Tasman sea, the sea existed between Zealandia and Australia in Gondwana stretching and break up. The sedimentary basin was infilled by fluvial and paralic sediments, including coal that forms the main source rock in the region (Fig. 2.4) (i.e. the Horse Range and Katiki formations; Uruski, 2010; Ghisetti and Sibson, 2012). The primary geometries and architecture of the basin are controlled by normal faults. The greatest subsidence occurred in the Clipper sub-basin, but widespread faulting created smaller grabens elsewhere (Fig. 2.3). This rifting period was related with final separation of New Zealand, Antarctica, and Australia during Gondwanaland break-up which had been starting in Jurassic. (Field and Browne, 1989)
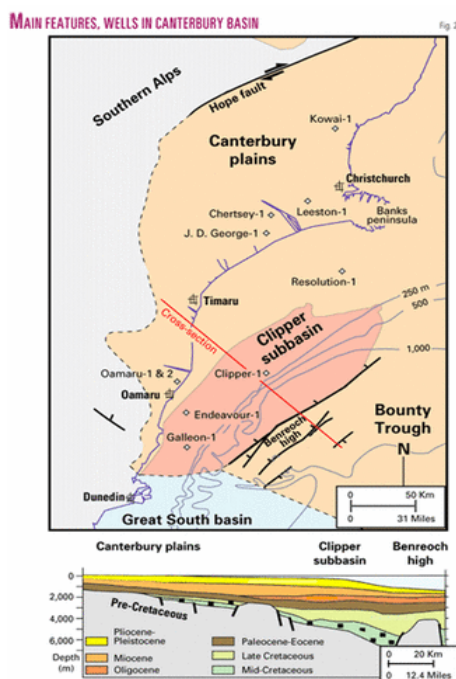
Fig. 2.3. The Clipper sub-basin where greatest subsidence occurred in the Canterbury basin (Sutherland and Browne, 2003).

Third, late Cretaceous passive subsidence occurred, resulting in transgression towards the northwest areas and another bulk subsidence of the basin until Paleocene. This characterised stratigraphically by the upwards progression from terrestrial sandstone and coal (i.e. the Pukeiwihai Formation) to deposition of marine sandstone, mudstone, and siltstone (Fig. 2.4) (i.e. the Katiki, Moreaki, and Hampden formations; Carter, 1988; Killops et al., 1997). Overlying these formations is the marine Amuri Limestone (Fig. 2.4) (Fulthorpe et al., 1996). In late Eocene, a new plate boundary propagated into New Zealand, but the Canterbury basin was outside the deformed region and continued to passively subside. Transgression reached its peak in Oligocene at ~29 Ma is marked in the Canterbury Basin by a regional unconformity (Fig. 2.4) (e.g., Carter, 1988; Fulthorpe et al., 1996).

Finally, late Oligocene to Recent deposition reflects progressive uplift and erosion of the Southern Alps, with resulting marine regression eastward and considerable sediment supply to the Canterbury basin, whilst the other bulk subsidence occurred in the Canterbury basin about 4-5 Ma ago as due to transcurrent tectonic of alpine (Fig. 2.4) (i.e. the 5 Tokama Siltstone; Lu et al., 2005)
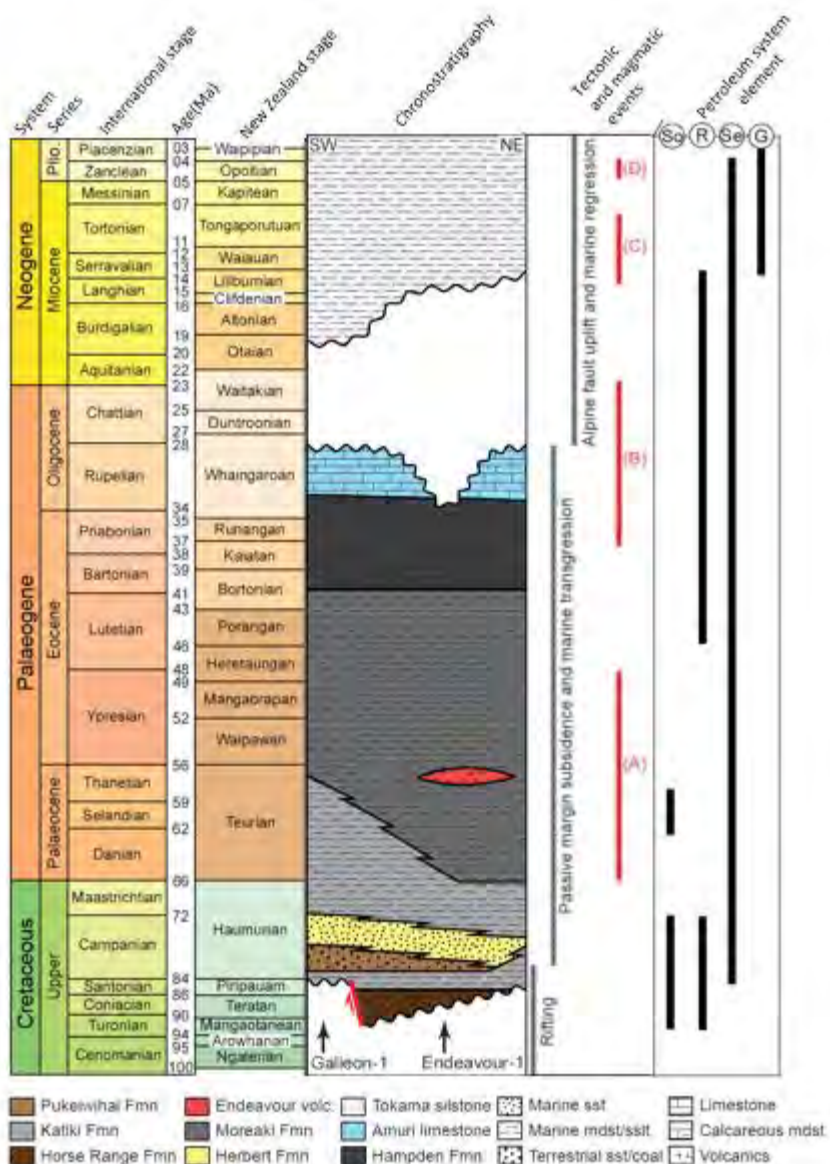
Fig. 2.4. Tectono-stratigraphic framework of the Canterbury Basin and phases of petroleum development derived from Reeves et al. (2017), highlighting ages of onshore magmatic events. Magmatic events correspond to: A = Geraldine and Timaru Lavas; B = Banks Peninsula; C = Cookson Volcanics; and D = View Hill, Central Canterbury (Timm et al., 2010). Petroleum system elements correspond to: So = source rock; R = reservoir rock; Se = Seal; and G = hydrocarbon generation.

2.3   The seismic stratigraphy and facies characterization of the Canterbury basin

Six broad seismic facies were derived and used to define sedimentary facies for the Cretaceous through Eocene succession by Sahoo et al. (2015). Six types of seismic facies are shown below and ordered from the top (younger age) of seismic image to the bottom (older age) respectively.

1) Bathyal (mainly mudstone) facies

These facies are observed in the Eocene section in all wells and consist of mudstone mainly. Plus, they are considered as regional seal rocks.

2) Shelfal (mudstone and siltstone) facies

Data from Clipper-1 show a wide range of depositional environments from shelfal to upper bathyal environments (Griffin, 2013) but there is no apparent distinction between environments based on seismic data. These facies are widely distributed from Late Cretaceous to the Eocene level.

3) Shoreface-shelfal (sandstone-siltstone) facies

They were widespread during Late Cretaceous - Late Paleocene. For the purpose petroleum modelling, they can act as the carrier beds or reservoir rocks.

4) Coastal sandstone and siltstone facies

They include deltas, estuaries and beach environments and dominate in Late Cretaceous.

5) Coastal coal measures facies

Coastal coal measures include coal and coaly mudstones which are the main source rocks in the study area (Shell BP Todd, 1984; Sykes and Funnell, 2002). They include deltas, estuaries and beach environments and widespread during mid Cretaceous.

6) Continental facies

In Mid-Cretaceous, sediments were deposited as alluvial fans and fluvial facies during rifting phase. Lacustrine facies might be possible in the isolated depocentres

with in syn-rift grabens; however, it is difficult to identify them by using seismic data alone.

2.4   The volcanism of the Canterbury basin

Intraplate igneous activity in Zealandia commenced in the Late Cretaceous (~100 Ma ago). Outcrops, wells, seismic reflection and magnetic data in the Canterbury basin show evidences of several igneous events occurring intermittently and locally from the Late Cretaceous to the Pleistocene and rock compositions vary from mafic to felsic as shown (Fig. 2.4 and Fig. 2.5) (Timm et al., 2010). For example, Miocene basaltic volcanoes that resulted in the Banks Peninsula and the Dunedin harbor located in the Canterbury basin are by far the largest of these features, but smaller intrusive and extrusive centers are widespread and have a variety of ages. (Sutherland and Browne, 2003).
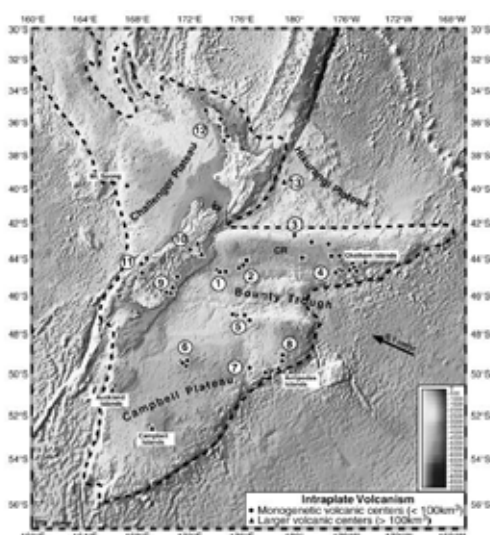
Fig. 2.5. Bathymetric map of the mainly submerged continent of Zealandia derived from Timm et al. (2010), outlined by the dashed line, and adjacent areas. Sampling sites are shown by black dots marking Cenozoic volcanic centers (monogenetic volcanic fields = circles and larger volcanic complexes/fields with ≥100 km3, including composite shield volcanoes = triangles). Sampling sites are (1) Urry Knolls, (2) Veryan Bank, (3) Graveyard seamounts, (4) western Chatham Rise, (5) northern Campbell Plateau margin, (6) Pukaki Bank, (7, 8) areas north and west of the Antipodes Islands, (9) Otago volcanic fields (including Timaru/Geraldine) and Dunedin Volcano, (10) Canterbury volcanic fields and Banks Peninsula, (11) Westland, (12) Auckland and Northland volcanic fields, and (13) Rowling B seamount on the Hikurangi Plateau. Plate motion vector is from Clouard and Bonneville (2005).
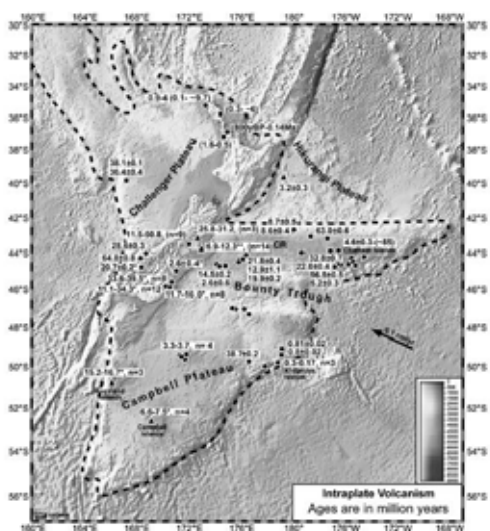
Fig. 2.6. The map of ages of intraplate volcanic centers of Zealandia derived from Timm et al. (2010). The Cenozoic volcanoes (black numbers) are irregularly scattered on the Central and Western Chatham Rise, the Campbell and Challenger Plateaus and the South and North Islands of New Zealand, showing no clear age progressions (symbols as in Fig. 2.5.). Age data from Hoernle et al. (2006) are marked with an asterisk, two asterisks refer to age data from Timm et al. (2009) and ages in brackets are taken from Cook et al. (2004) and Smith et al. (1993).

Chapter 3

Methodology

3.1   Data and software employed in the study

The study was conducted by using geophysics tools and the following 3 main data below.

1.   3D volume seismic reflection dataset of WAKA 3D

2.   2D line seismic reflection dataset of TIE1P1

3.   Galleon-1 well data

All data were derived in the Canterbury basin. The 3D seismic volume (Waka3D block) has an available recording length of approximately 4.8 s (Two Way Time) and a bin spacing of 12.5 m x 25 m in crossline and inline directions respectively. The seismic volume is a post-stack where acoustic impedance increases are indicated by positive amplitudes, and dominated by frequency of 30-50 Hz, resulting in a vertical resolution of about 10.0-16.7 m, using an average sediment velocity of 2.0 km/s and the horizontal resolution of about 20.0-33.4 m. These ensure confidence in geomorphological interpretation of the igneous intrusions. Plus, 2D line seismic reflection datasets were also employed to extend the interpretation from the Galleon-1 well that was drilled outside of 3D seismic survey to correlate lithostratigraphy in the study area (Fig. 3.1.). Seismic interpretation was conducted in Petrel2013 software.
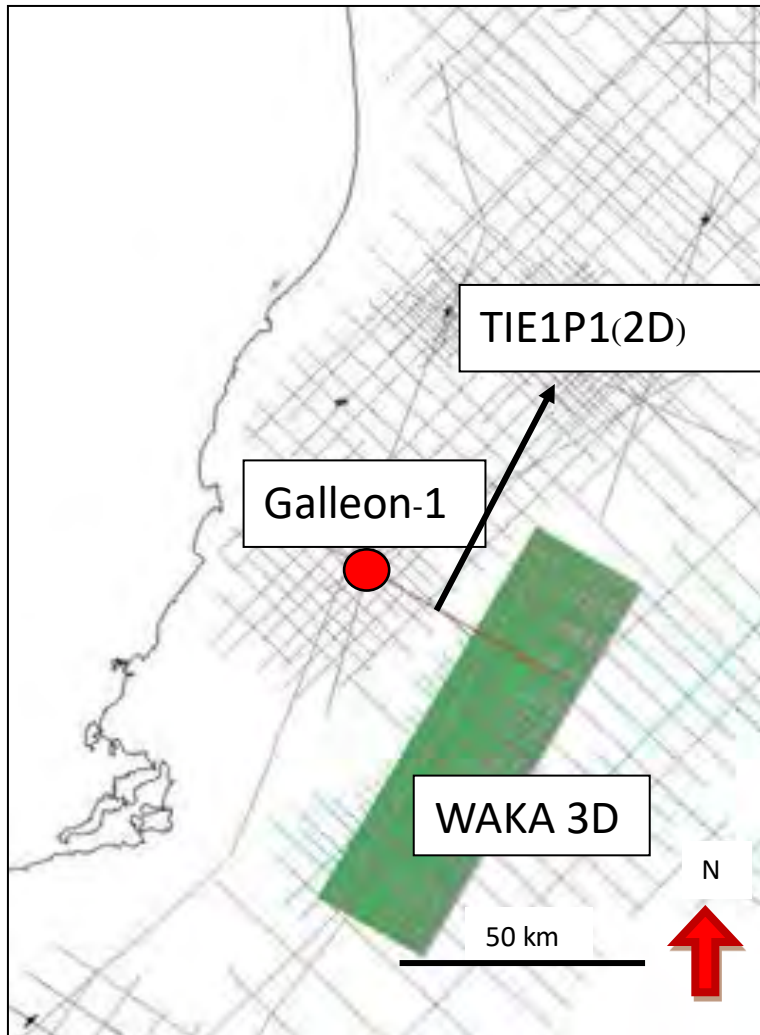
Fig. 3.1. Three main data employed in the study within the Canterbury basin on the east coast of southern island, New Zealand.

3.2   Seismic interpretation

Studying igneous intrusions in subsurface starts with detecting all potential igneous intrusions in the 3D seismic reflection data. There are common criteria which are employed to interpret seismic reflections of igneous intrusions and make the interpretation more reliable and accurate. Commonly, seismic reflections of igneous intrusions show apparently high amplitudes due to the high contrast of acoustic impedance values between igneous intrusions and surrounding rocks which mostly are sedimentary rocks. Plus, seismic reflections of igneous intrusions transgress and intrude locally in seismic profiles. Lastly, they tend to terminate abruptly. An example of seismic reflection data satisfying criteria is showed (Fig. 3.2).
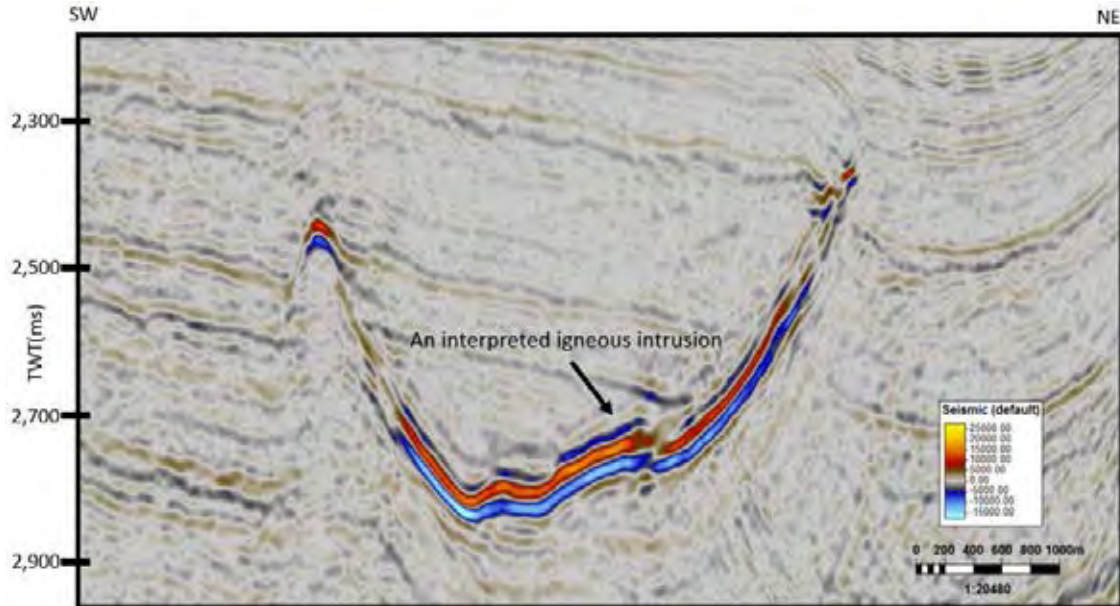
Fig. 3.2. The seismic reflection satisfying criteria and interpreted as an igneous intrusion.

Consequently, the very first thing to do is searching for seismic reflections that satisfy these criteria throughout the study area (Waka 3D). However, some might not satisfy all the criteria completely, so it means that interpretation would be less reliable and accurate. Then, each igneous intrusion will be detected and visualized or imaged by 2 methods mentioned in the next item. After visualizing all seismic reflections of igneous intrusions throughout the study area, they must be described in aspects of seismic characteristics, distribution and geometry as results of the study. The description will benefit inferring potential feeders and magma flow patterns and directions and the effects of igneous intrusions on surrounding rocks such as forced fold (domal uplift) of sedimentary rocks overlying the intrusions.

3.3   Methods of imaging seismic reflections of igneous intrusions

3.3.1   Surface generation

After seismic reflections of igneous intrusions satisfy the criteria mentioned above and are considered as igneous intrusions. Then, seismic reflection tracking is applied to track seismic reflections of all possible igneous intrusions existing in seismic profiles.

Next, the surface of igneous intrusions will be generated from the tracking (Fig. 3.3). However, the software automatically makes the interpolation of the surfaces of igneous intrusions, so the gap where there is no seismic reflection satisfying igneous intrusions will be filled up. Accordingly, the surfaces derived might not represent the totally exact igneous intrusions.
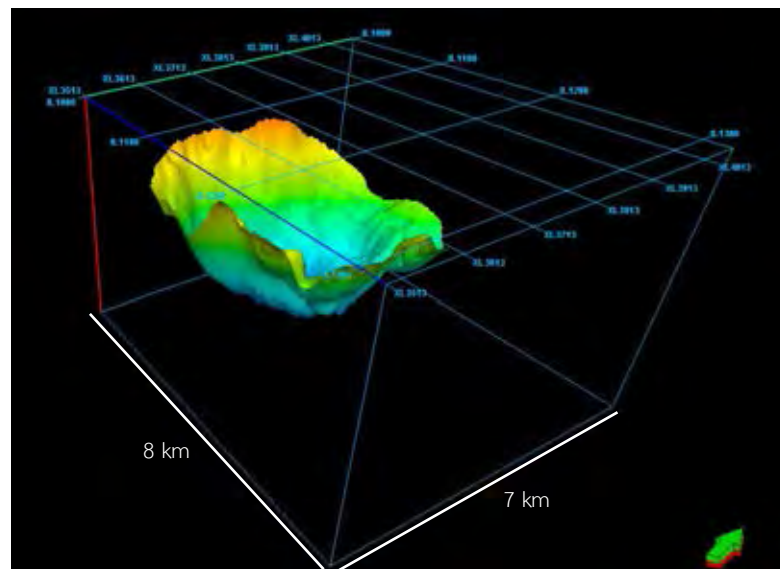
Fig. 3.3. The surface of an igneous intrusion generated by tracking the seismic reflection of the igneous intrusion.

3.3.2   Geo-body extraction

Geo-body extraction is one of the effective and popular visualizing methods among earth scientists studying igneous intrusions. Firstly, surface mapping of igneous intrusions gives the rough understanding of how and where igneous intrusions were located and distributed throughout the study area. Then, box probe will be used to cut off unwanted parts and keep the interesting parts of total 3D seismic datasets, so the boxes created in the parts where surfaces of igneous intrusions exist. Each box covers total surfaces of igneous intrusions to ensure whole seismic reflections of igneous intrusions lay in the box. (Fig. 3.4a, Fig. 3.4b and Fig. 3.5).
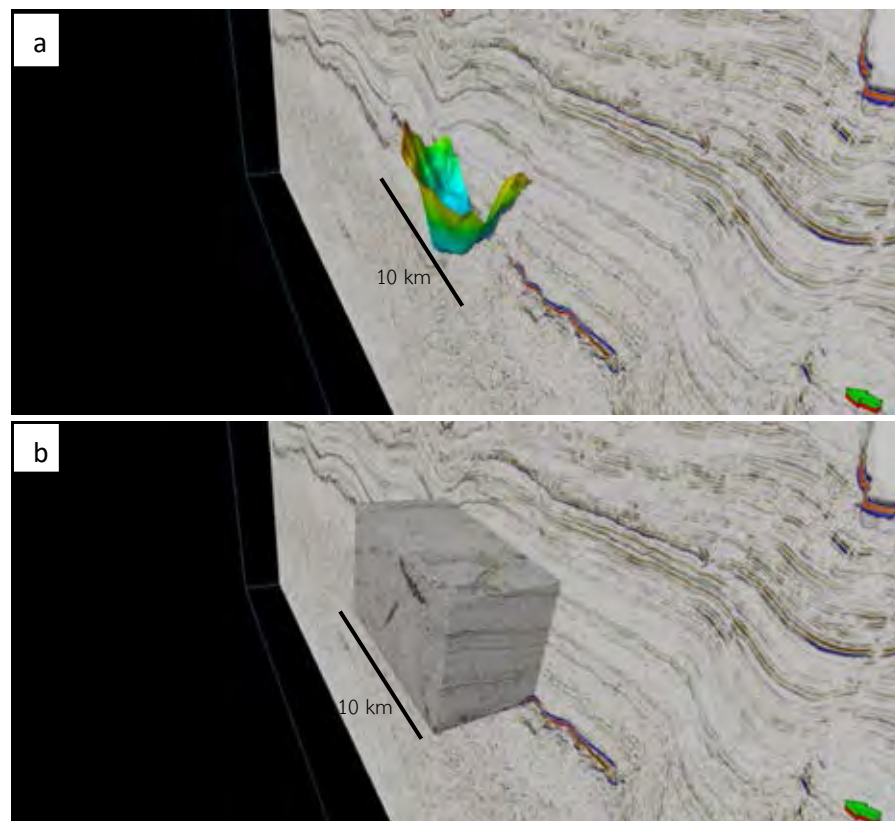
Fig.3.4. (a) The surface of an igneous intrusion helping to create the box probe covering the total igneous intrusion. (b) The generated box probe to cover the surface of the igneous intrusion.
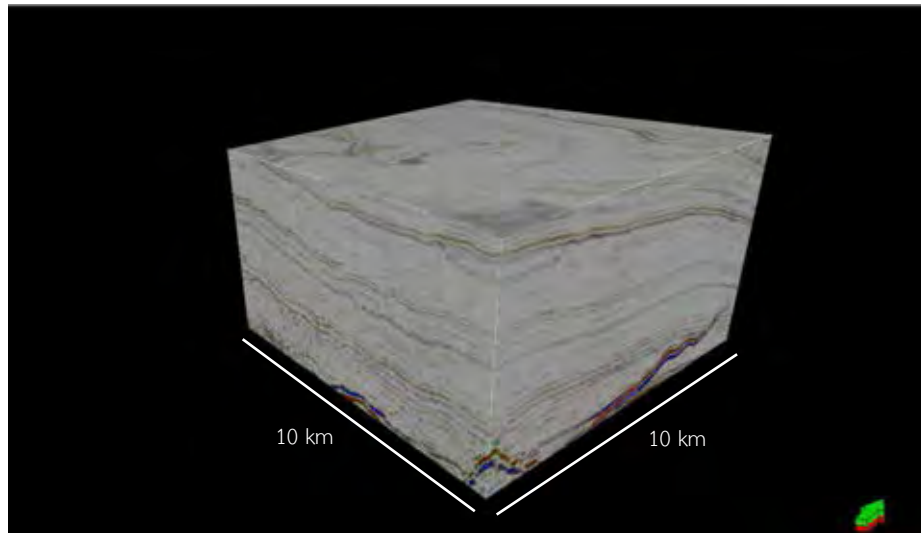
Fig.3.5. The box probe covering the surface of the igneous intrusion, showed in 3D.

Next, amplitude extraction will be employed to extract only strong amplitude seismic by applying the RMS (root mean square) attribute (Fig. 3.6). This attribute is applied to amplify and increase the contrast between the strong amplitude seismic reflections and the weak amplitude of surrounding ones.
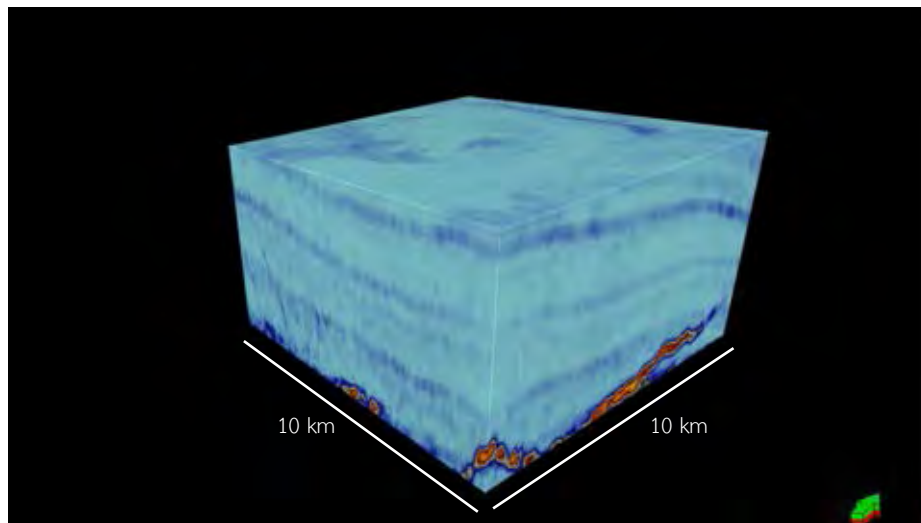
Fig.3.6. The box probe applied the RMS attribute to amplify the contrast between the strong amplitude ones and the weak ones.

Then, opacity rendering is used to make the strong seismic reflections representing igneous intrusions opaque and colored; moreover, it turns the surrounding to become transparent. Consequently, the geo-body of total exact seismic reflections representing igneous intrusions will be derived and visualized in 3D (Fig. 3.7). Additionally, sculpturing could be applied to get more correct and better image (Fig. 3.8). by cutting off some unreliable seismic reflections.
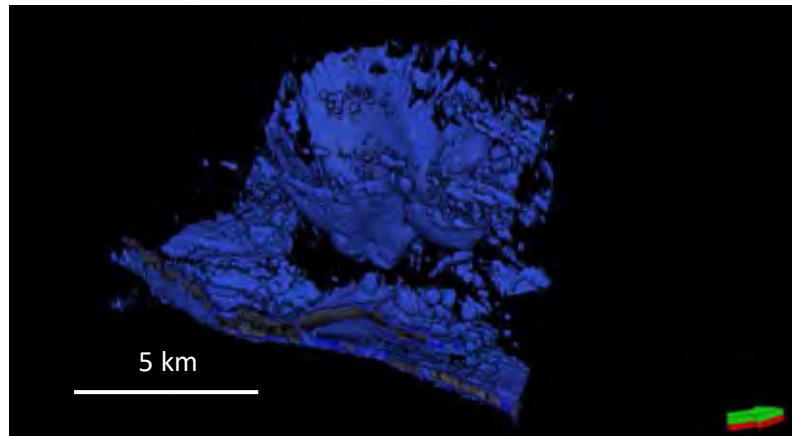
Fig.3.7. The geo-body of an igneous intrusion before sculpturing.
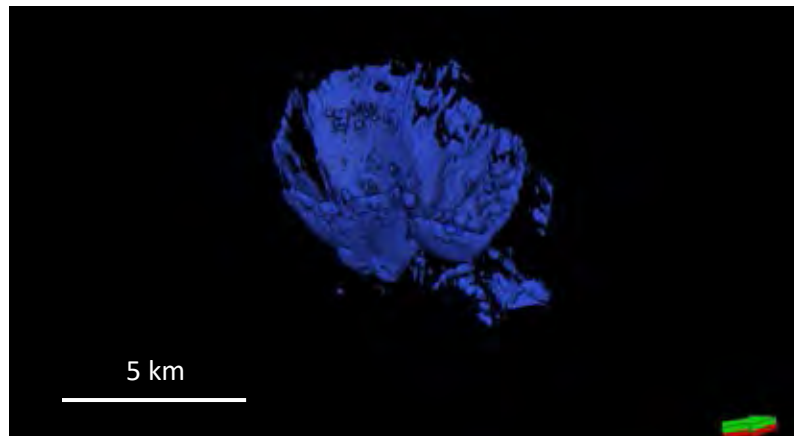
Fig.3.8. The geo-body of the igneous intrusion that was sculpted.

3.4   Well data correlation

The age relationship between igneous intrusions and host rock formations can be derived reliably from well data correlation. This method provides the correlation between tangible data which are well data and intangible data which are seismic data. However, there is no well appearing in the 3D seismic data used, so the best and nearest well which is the Galleon-1 well will be used. Commonly, there are some 2D seismic lines passing through both well and 3D seismic volume for benefits of correlation. Firstly, 2D seismic line passing through both WAKA 3D and Galleon-1 will be loaded along with Galleon-1 well data (Fig. 3.9). Rock formations will be presented in the well section incorrectly in the first place. Because the depth measurement scale of seismic data is in TWT (two-way-time) whilst the depth measurement scale of well data is in meters, so it requires the seismic well tie to correct this problem.
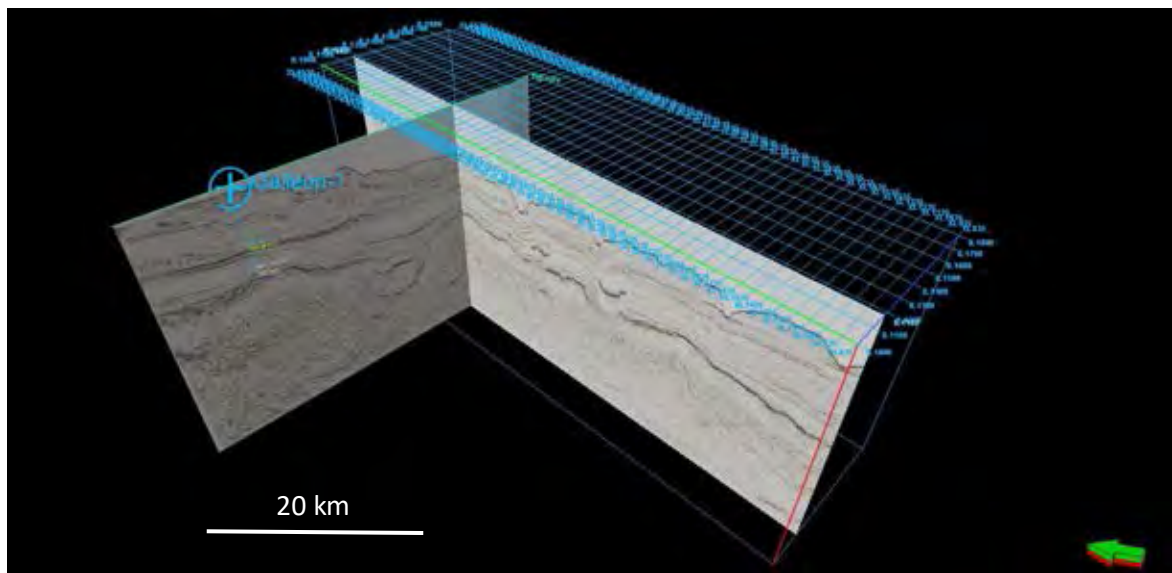
Fig.3.9. The window of 3D seismic volume and 2D seismic line and Galleon-1 well data.

Seismic well tie

It is the process providing synthetic seismogram calibrated to seismic data to acquire the depth in the unit of meters instead of two-way-time. To generate synthetic seismogram, two main wire line log data are needed; sonic log data providing wave velocity through formations, density log data providing density of rock formations. Then acoustic impedance of each formation is calculated by the product of multiplying compressional wave velocity and density of a formation. The values of acoustic impedance are used to determine reflection coefficient to do convolution with wavelet of seismic data. So, synthetic seismogram is derived (Fig. 3.10). The synthetic seismogram will be calibrated to seismic data by shifting synthetic seismogram to correlate to seismic data. Finally, the depth level in meters of each rock formation is derived in the well.
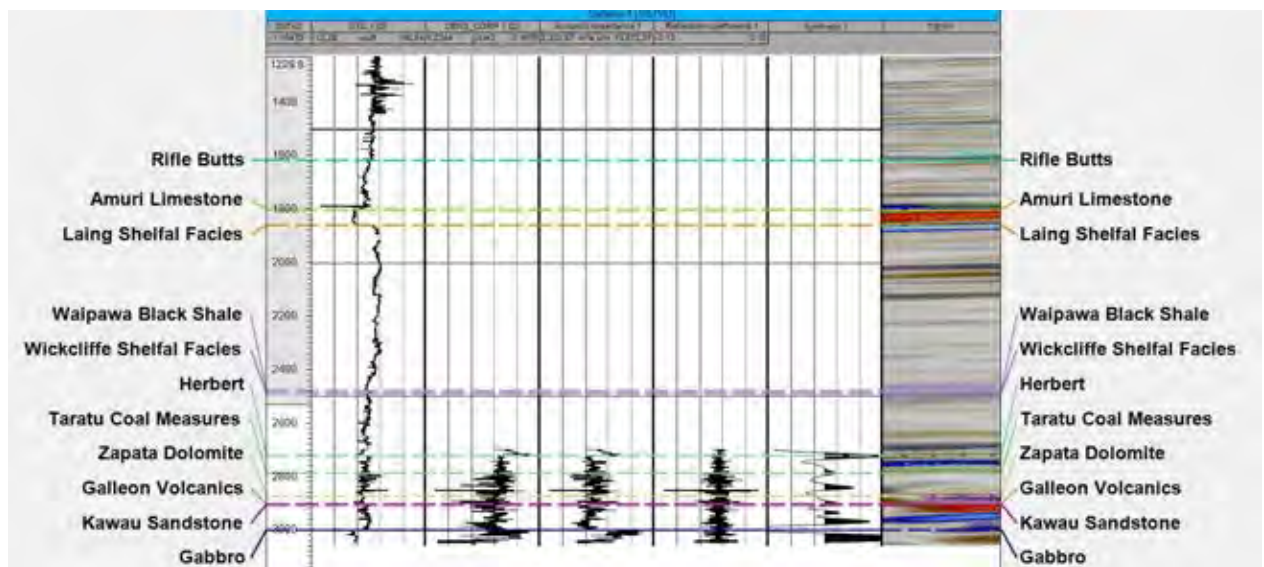
Fig.3.10. The columns of compressional velocity, density, acoustic impedance, reflection coefficient, synthetic seismogram and seismic data (left to right) respectively with rock formations.

After deriving known tops of rock formations correlated to 2D seismic line, the seismic reflection lines of each top formations will be tracked to correlate to 3D seismic volume (Fig. 3.11.). Finally, horizons of each top of rock formations will be created by tracking and used to correlate to the emplacement timing of igneous intrusions.
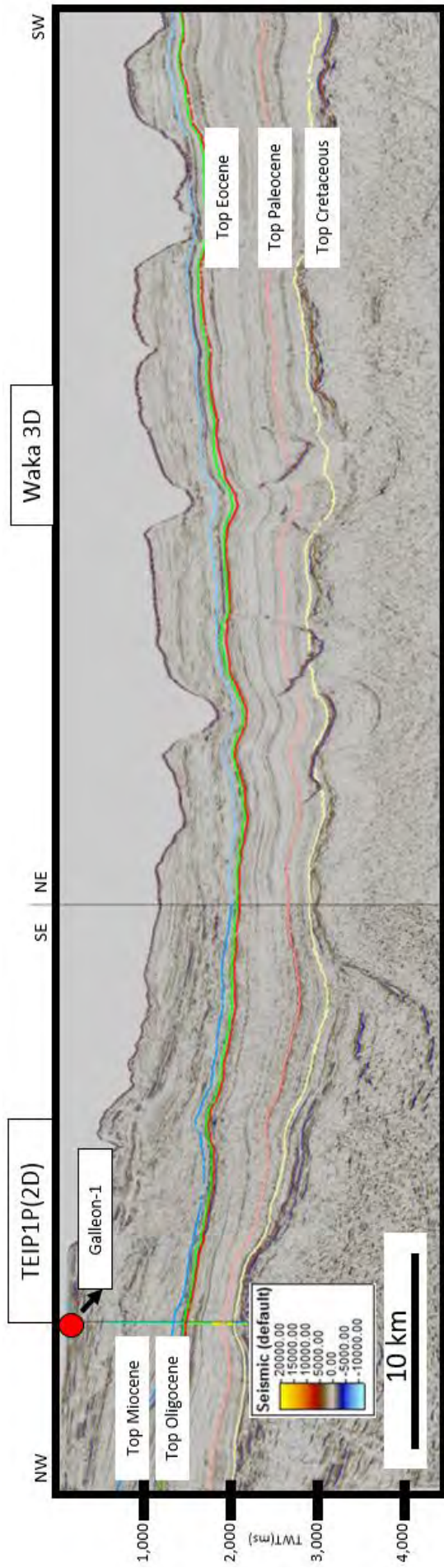
Fig.3.11. Tracking horizon in 3D seismic volumes by correlating to 2D seismic data and well data.

Chapter 4

Results

There are 3 main results described in the study, including the location and distribution of igneous intrusions, the seismic characteristics and geometries of igneous intrusions and the relative age between igneous intrusions and host rock formation as follows.

4.1   The location and distribution of igneous intrusions

The study shows that there are 5 possible igneous intrusion bodies in the study area, covering a total area of at least 80 square kilometers (Fig. 4.1a and Fig. 4.1b). On the map view, most of the igneous intrusions are located and distributed nearby in one another on the west center of WAKA3D. However, the fifth sill unit (igneous intrusion unit) is located far away from the others. Sill unit 1 to sill unit 4 are roughly at the same depth level (TWT) whilst sill unit 5 is at the deeper level, the cooler color is, the deeper igneous intrusion is.
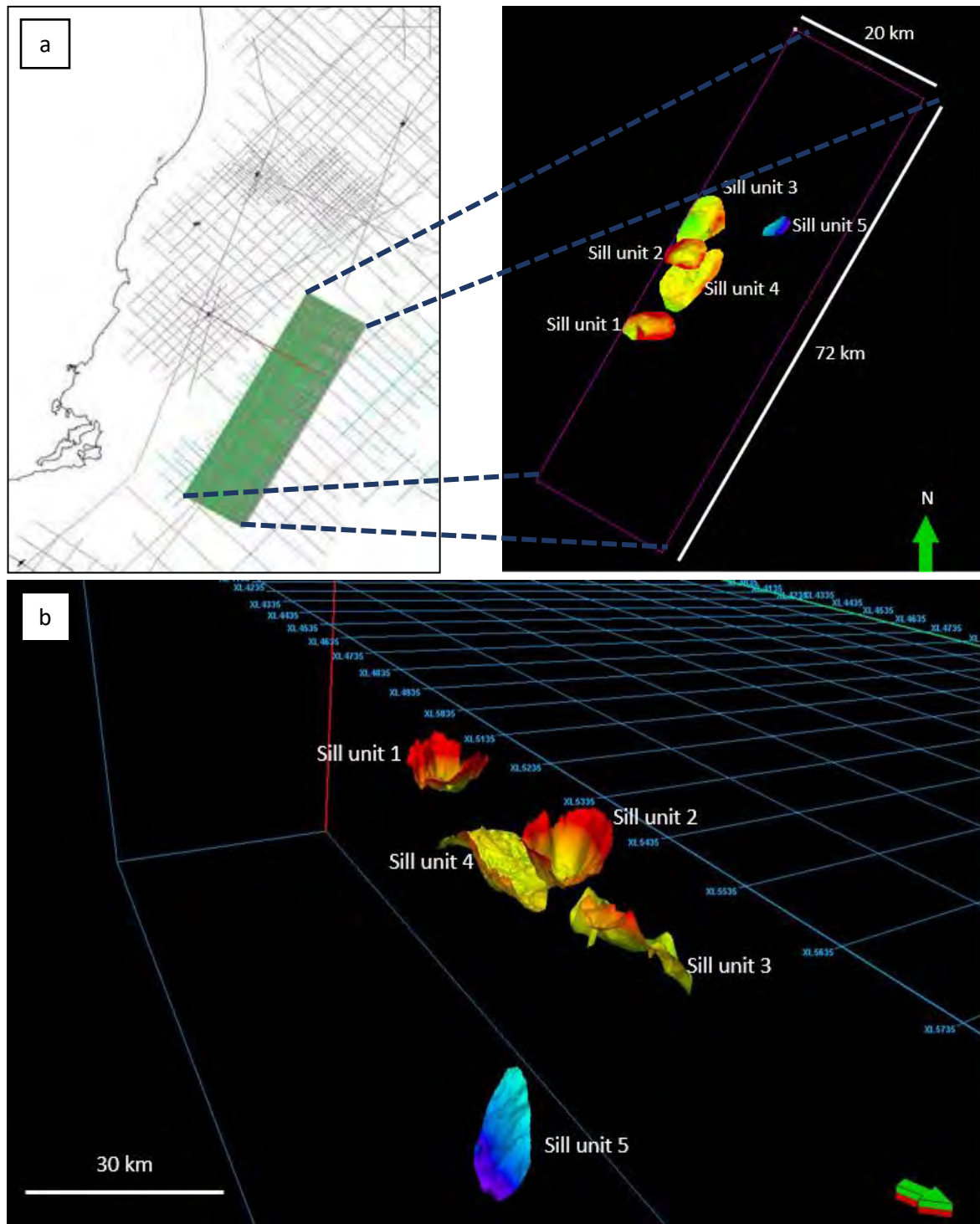
Fig. 4.1. (a) The bird's eye view map of the study area showing igneous intrusions. (b) The 3D view map of the study area showing all sill units.

4.2   Seismic characteristics and geometries of igneous intrusions

The shapes of five sill units are different from one another. Consequently, they are divided into 3 main types; a saucer-shaped sill, an inclined sheet and a layer-parallel sheet. To make general description and get the better understanding of each sill unit, the methods of measurement are defined as follows.

4.2.1   Measurement methods of geo-body size

There are 3 main types of igneous intrusions occurring in the study area: a saucer shaped sill, an inclined sheet, a layer-parallel sheet. The description table shows how to measure length of any geometries of igneous intrusions (Fig. 4.2).

X-section view	Top view	Geometry/Measurement
		Saucer shaped sill H = Height L = Long-axis length S = Short-axis length
		Inclined sheet H = Height L = Length W = Width
		Layer-parallel sheet L = Long-axis length S = Short-axis length
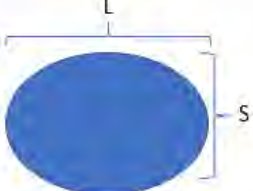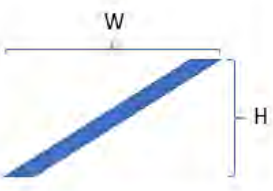
Fig. 4.2. The description table showing how to measure length of any geometries of igneous intrusions ideally.

4.2.2 The description of each sill unit

a. Sill unit 1

The seismic reflections is interpreted as an igneous intrusion and characterized by high amplitude, medium to low frequency and low continuity (Fig. 4.3). The 2D shape of the body is cancave upward. The average height of this body is 550 milliseconds (TWT) and the angle of the inclined sill to the horizon is steep. It is noticed that seismic reflections under interpreted igneous body are unclear. Furthermore, the weaker amplitude seismic reflections interpreted as sedimentary layers overlying this igneous body are convex upward. Sill unit 1 covers an area of about 17.97 km^2 (Fig. 4.4).
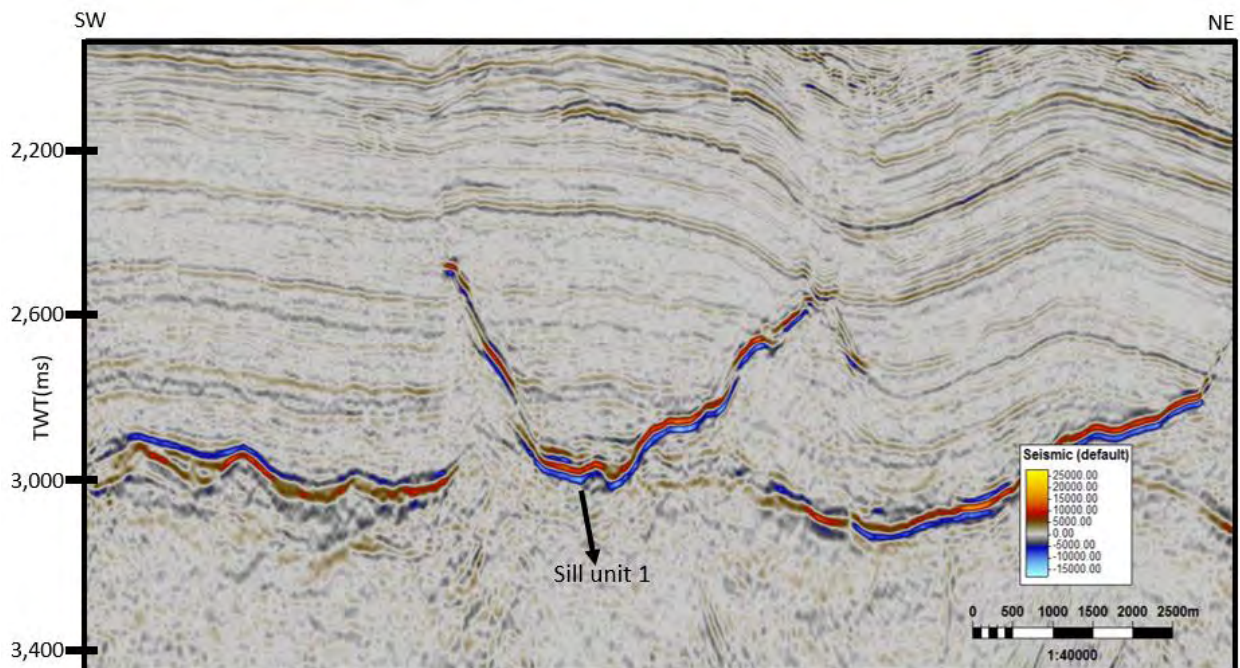
Fig. 4.3. The seismic reflection profile showing sill unit 1 (at the center).
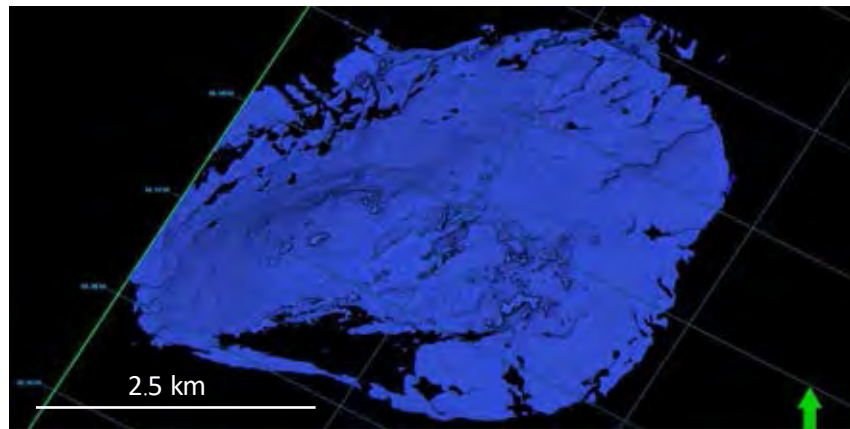
Fig. 4.4. The top view of geo-body of sill unit 1.

In the 3D seismic window (Fig. 4.5) after rendering geo body extraction, the shape of this igneous intrusion is like saucer; thus, it is called "saucer-shaped sill". The igneous body looks almost elliptically symmetric. Consequently, it is divided in to 3 main parts; the inner sill located at the center of the body, the outer sill or inclined sheet connecting with the inner sill and dendritic rim on which discontinuity of the body can be seen easily. The long and short-axis lengths of this body are approximately 3 and 2 kilometers respectively. However, there is a big gap or discontinuity in the inclined sheet in south of this igneous body.
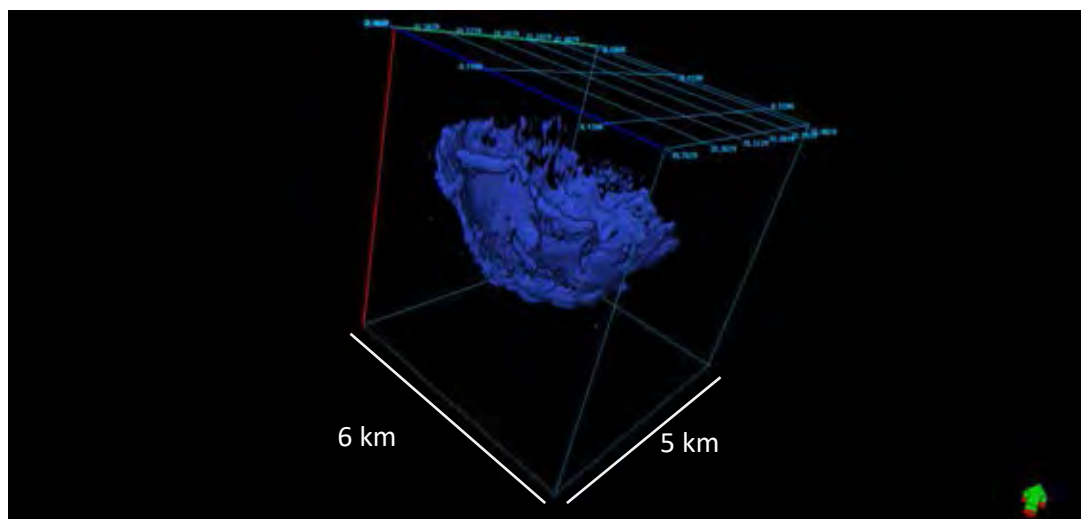
Fig. 4.5. The 3D geo-body of sill unit 1.

b. Sill unit 2

This sill unit is characterized by high amplitude, medium frequency and low continuity. It intruded the horizontal seismic reflections as inclined or dyke like intrusion which is distal to the basement (Fig. 4.6). The dyke-like intrusion has the height of 500 milliseconds and make a steep angle to the horizon. Sill unit 2 covers an area of about 21.18 km^2 (Fig. 4.7).
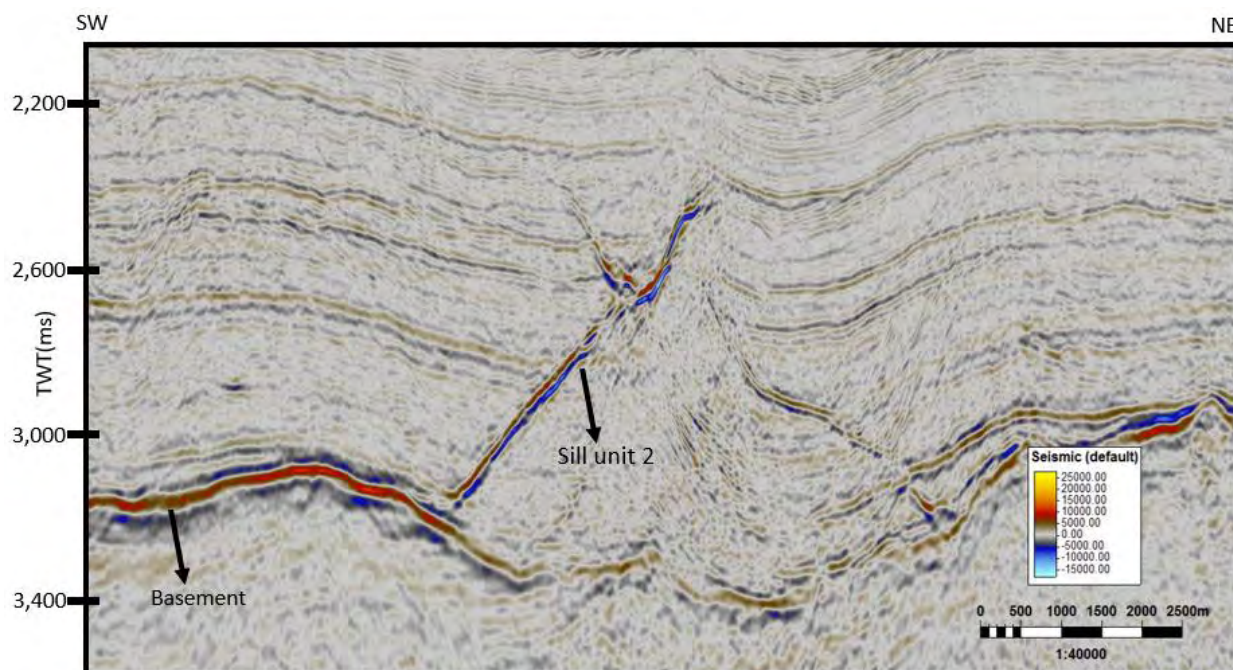

Fig. 4.6. The seismic reflection profile showing sill unit 2 (at the center).
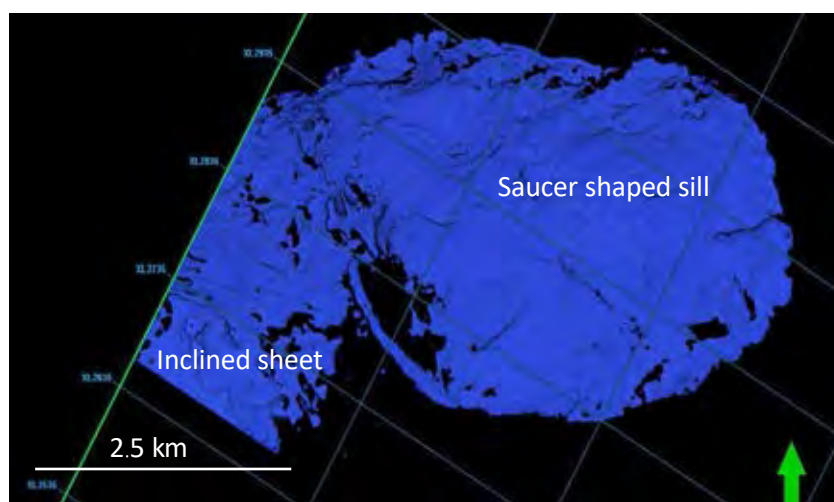
Fig. 4.7. The top view of geo-body of sill unit 2.

However,in 3D seismic volume at IL 1260, the shape of igneous intrusion turned to be concave upward (Fig. 4.8). Additionally, the weaker amplitude seismic reflections above this igneous body are convex upward. The width and height of this intrusion in the picture is around 2.8 kilometers and 300 ms respectively.
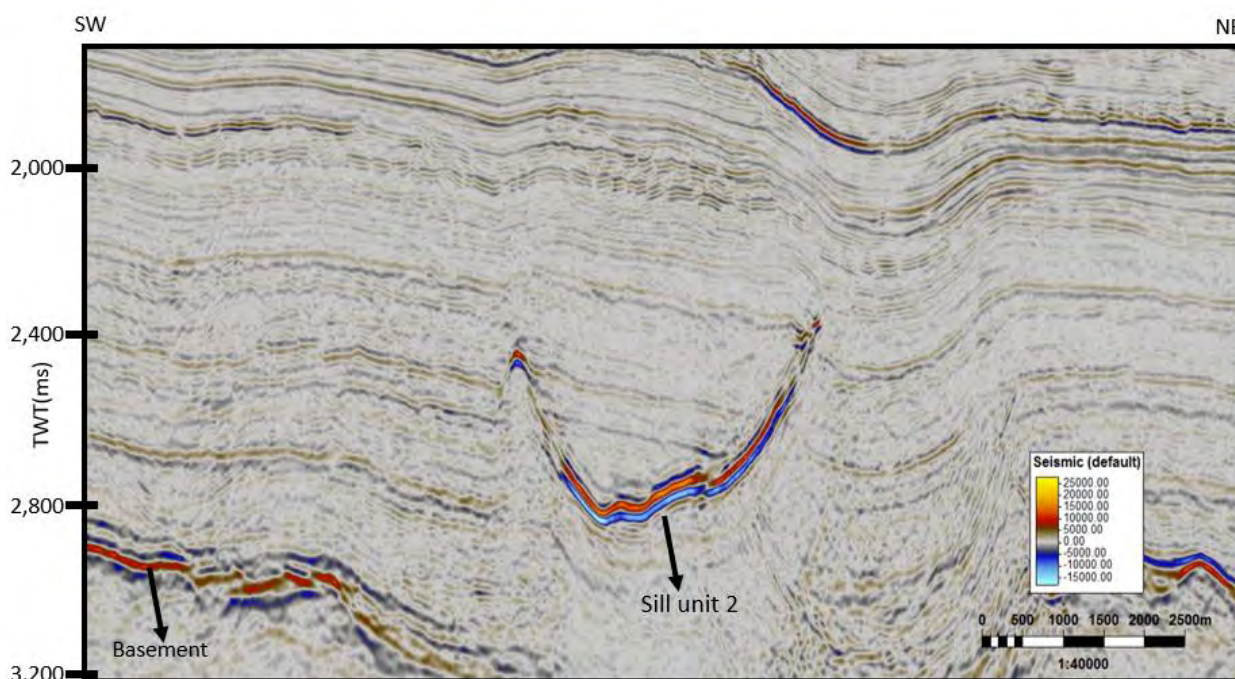
Fig. 4.8. Another seismic reflection profile showing sill unit 2 (at the center).

By rendering the same technique, the 3D shape of the igneous body is quite complex; thus, it is called "complex sill" which is supposed to form due to hybridization of magma intrusions (Fig. 4.9). It consists of a saucer-shaped sill and an inclined sheet connected to one another. The long and short-axis lengths of saucer-shaped sill are 1.7 and 2.8 kilometers respectively. Whatsoever, the length of the inclined sheet is obscure. As there are no available seismic reflection data connected to it at the lowest bottom and it is connected to the basement where seismic reflections are very dim and messy, termination of the igneous rock cannot be seen.
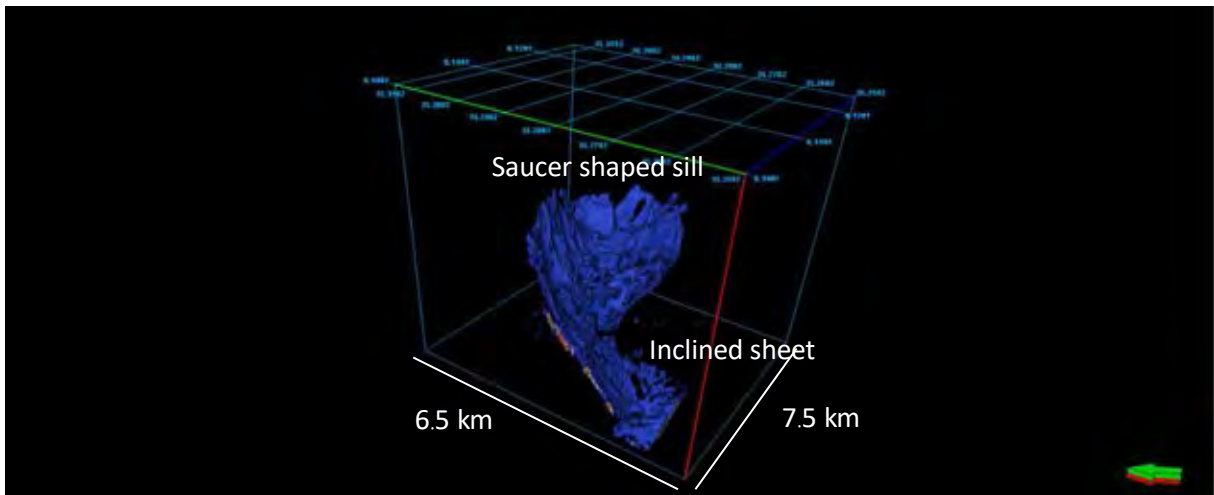
Fig. 4.9. The 3D geo-body of sill unit 2.

c. Sill unit 3

Seismic characteristics of the sill are high amplitude, low frequency, meduim continuity (Fig. 4.10). There are 2 igneous intrusions closed to the basement showing high amplitude. The right one is smaller than the left one (Fig. 4.10). However, the 2D shape of both intrusions is concave upward. Plus, the seismic reflections above these intrusions, which are weaker, are concave upward as these intrusions are. Sill unit 3 covers an area of about 17.31 km^2 (Fig. 4.11).
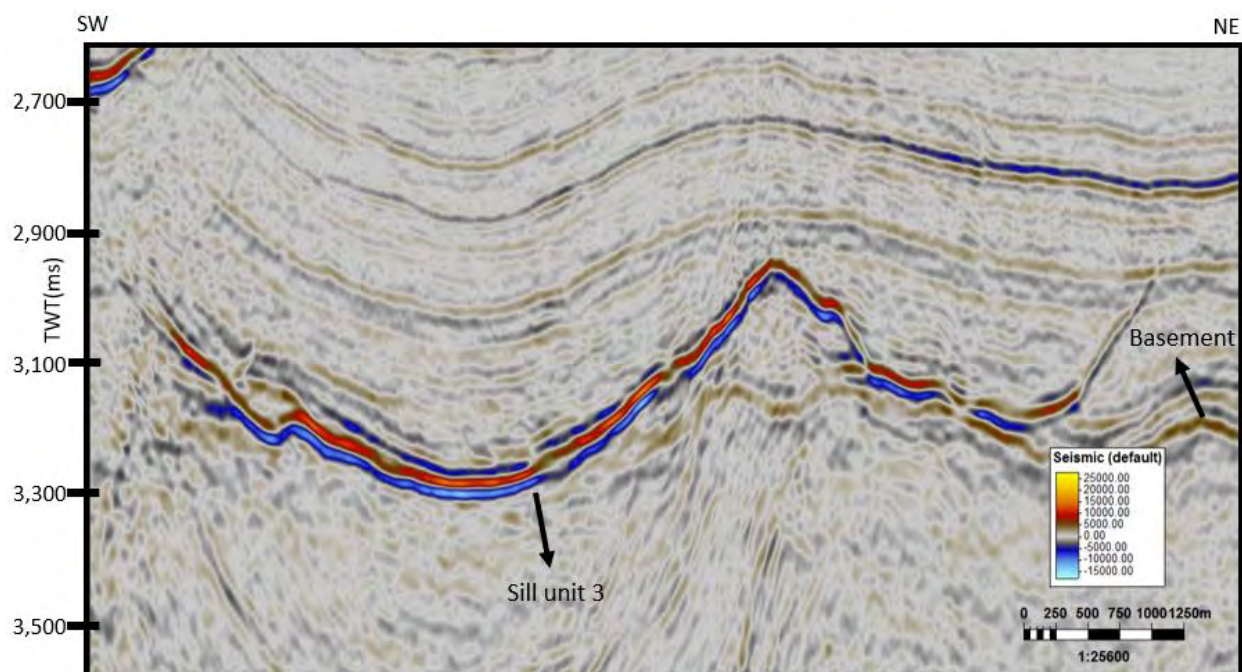
Fig. 4.10. The seismic reflection profile showing sill unit 3 (in the red dot rectangle).
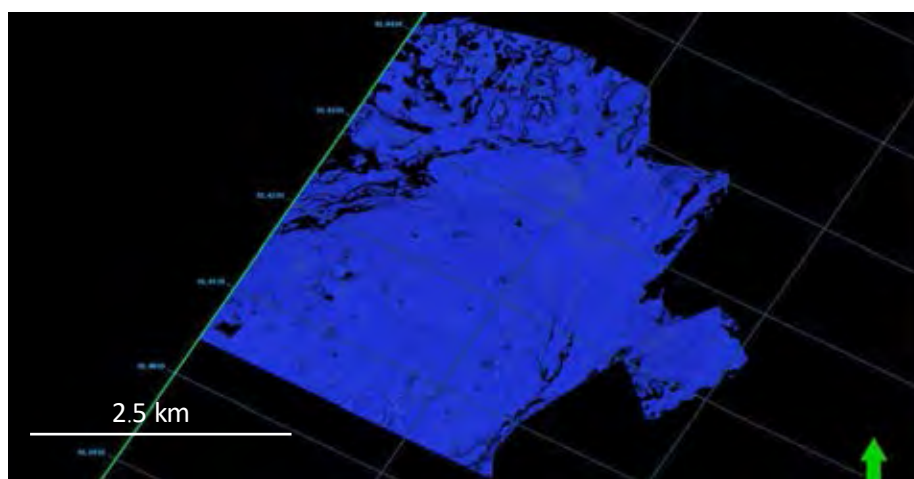
Fig. 4.11. The top view of geo-body of sill unit 3.

By rendering the same technique, the 3D shape of the igneous body is inclined sheet (Fig. 4.12). The smaller inclined sheet (on the left side of the picture) is dipping roughly northward whilst the larger one is dipping southward and has the height of 250 ms. On map view, the size of the length of smaller and larger inclined sheets are 2 and 9 kilometers.

However, there are no available seismic data for the termination of the larger inclined sheet, so the width is unclear.
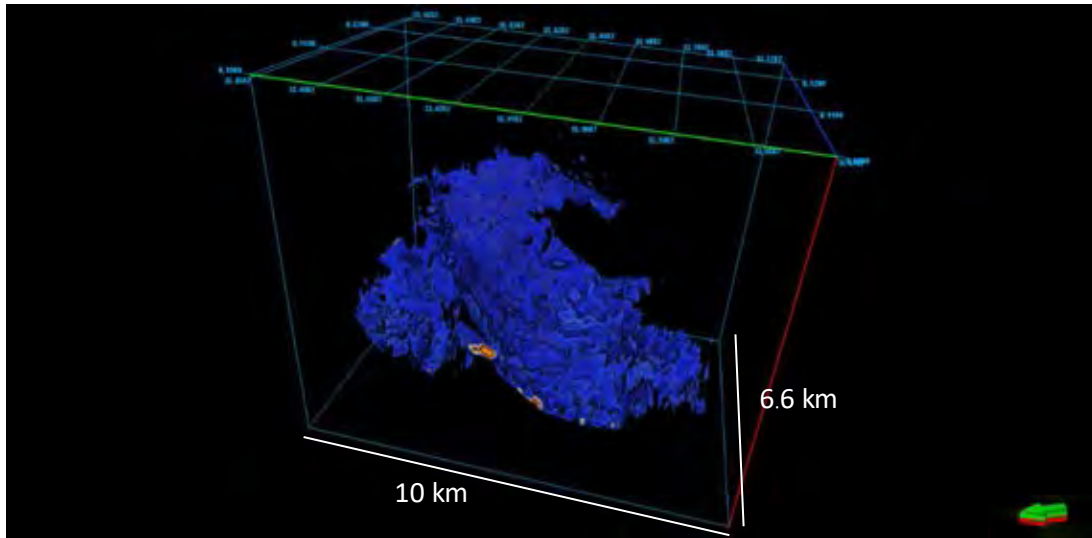
Fig. 4.12. The 3D geo-body of sill unit 3.

d. Sill unit 4

This interpreted sill is a reflection of high amplitude, low frequency and medium continuity. There is a igneous intrusion closed to the basement (Fig. 4.13). This intrusion seems slightly concave upward; however, it is sub-horizontal in most Inline profiles. Plus, the seismic reflections above this intrusion, which are weaker in amplitude, oriented horizontally.
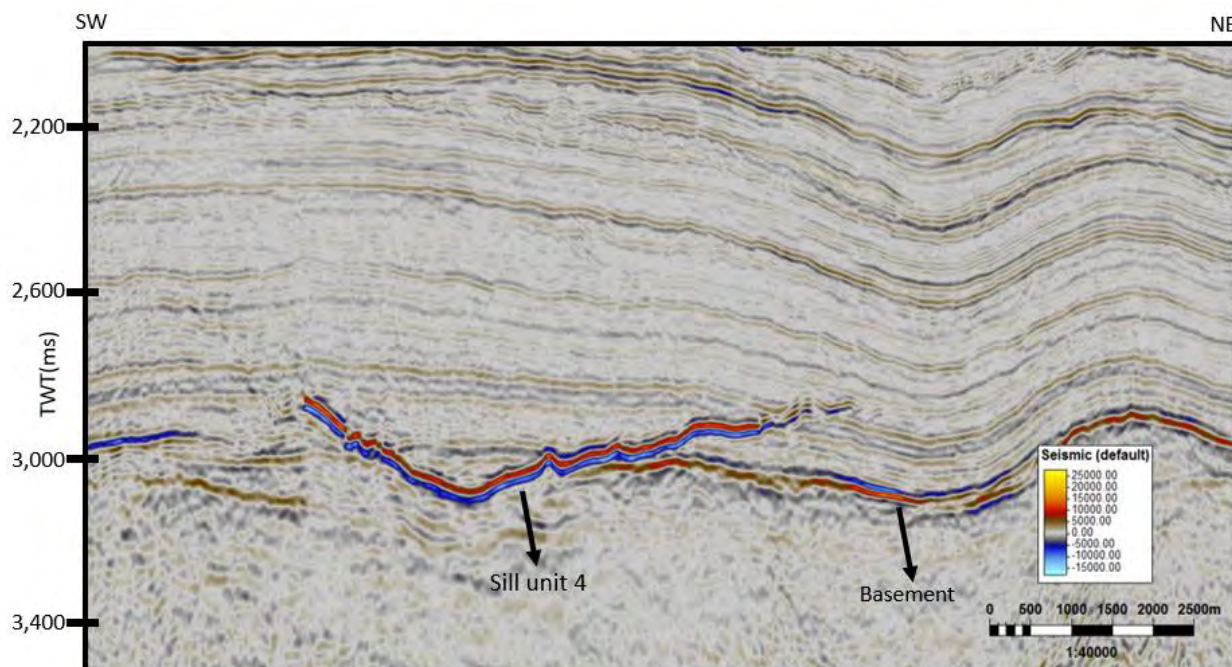
Fig. 4.13. The seismic reflection profile showing sill unit 4 (at the center).

From geo-bodies (Fig. 4.14), there are 2 main shapes of sills including an inclined sheet and a layer-parallel sheet or sub-horizontal sheet. Consequently, the combination of 2 shapes of igneous intrusion is called "complex sill". Plus, the angle of the inclined sheet is steep and the height is 600 milliseconds (measured in XL 3660), whilst the layer parallel sill seems insignificantly convex upward.
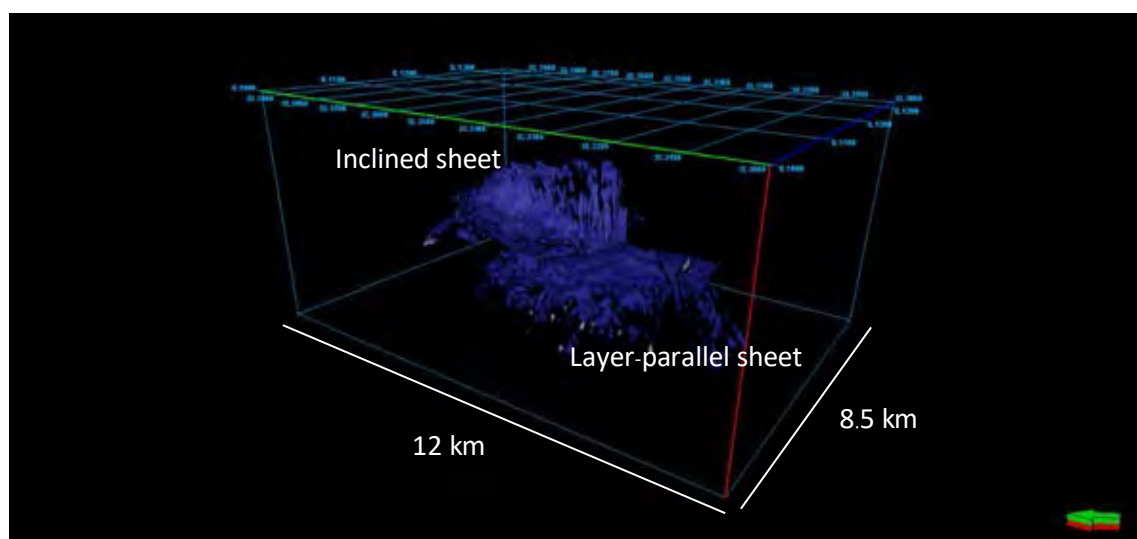
Fig. 4.14. The 3D geo-body of sill unit 4.

Sill unit 4 covers an area of about 33.43 km^2 (Fig. 4.15). The layer-parallel sill has the long-axis length is 4.4 kilometers and the short axis length is 2.7 kilometers. The length of the inclined sheet is 6.0 kilometers and the width is 2.4 kilometers.
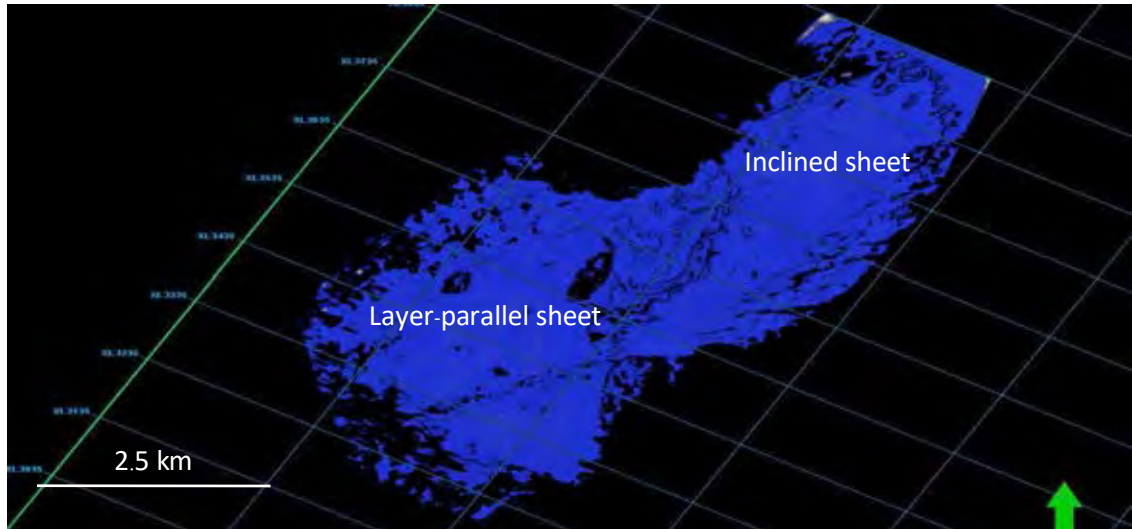
Fig. 4.15. The top view of geo-body of sill unit 4.

e. Sill unit 5

Under the basement, seismic characteristics of this sill are medium to high amplitude (Fig. 4.16). The seismic reflections are messy and weak; however, there are the seismic reflections expressing stronger amplitude than that of surroundings. The strong amplitude seismic reflections mentioned are slightly inclined and make a small angle to horizon. Plus, the vertical height is 200 milliseconds. Sill unit 5 covers an area of about 3.81 km^2 (Fig. 4.17).
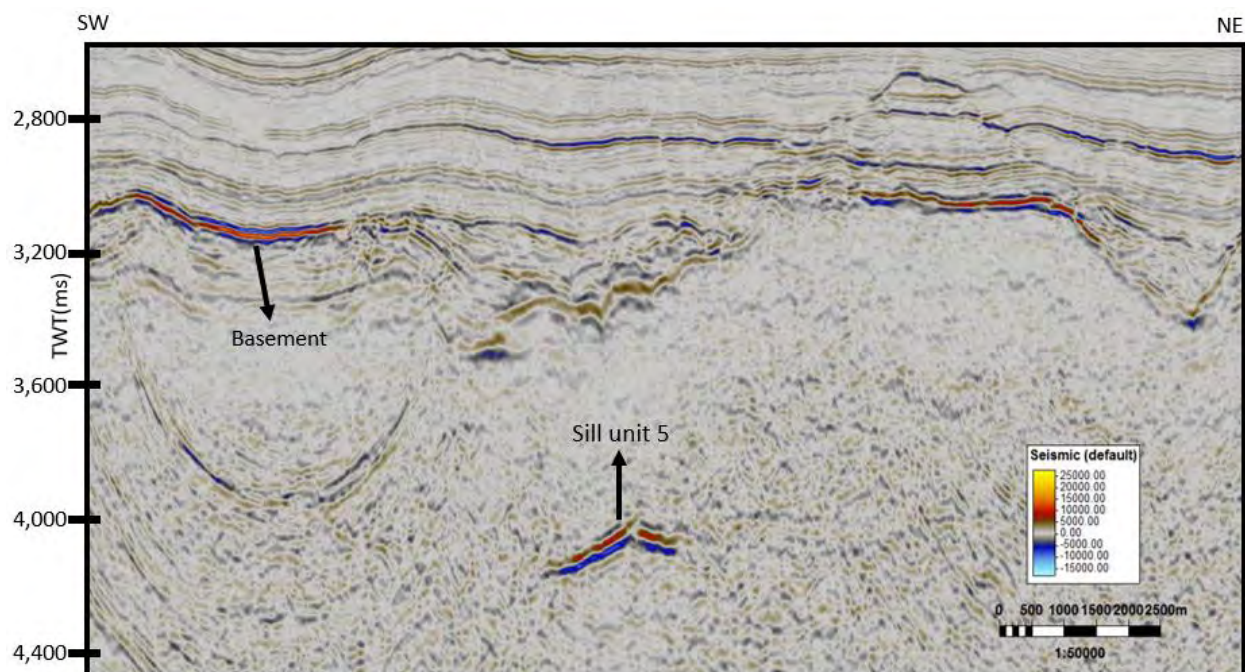
Fig. 4.16. The seismic reflection profile showing sill unit 5 (at the center of the bottom).
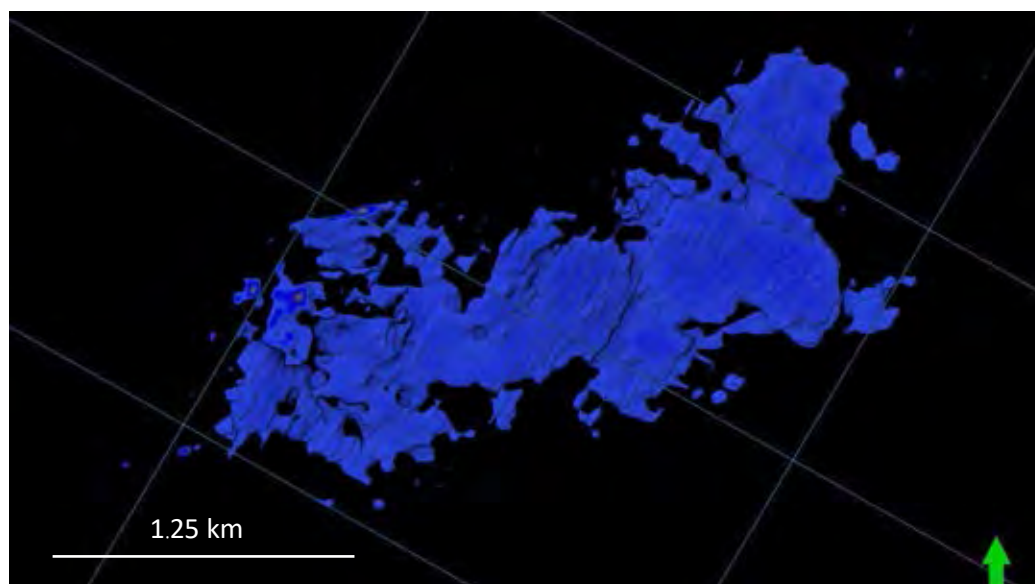
Fig. 4.17. The top view of geo-body of sill unit 5.

The igneous intrusion has a inclined sheet morphology and is discontinuous or patchy (Fig. 4.18). The geo-body is inclined and make a small angle to horizon. The average length is 750 meters. Plus, the height and the width are 200 milliseconds and 1 kilometers respectively.
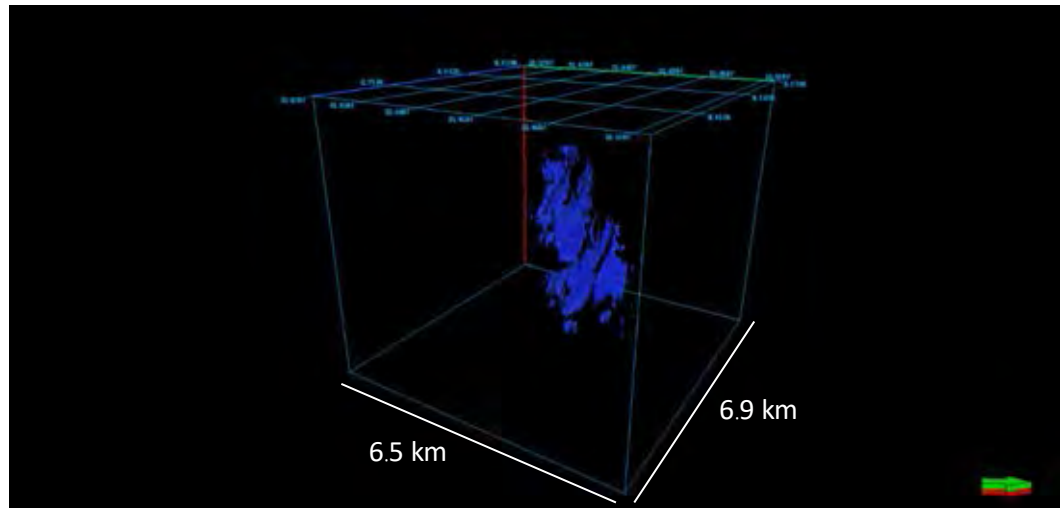
Fig. 4.18. The 3D geo-body of sill unit 5.

4.3   The relative age between host rock formations and igneous intrusions

Well data of Galleon-1 provided the tangible data of ages of rock formation. This leads to correlation of well data to seismic data. Consequently, the interpreted horizons represent tops of the host rock formations at any ages. All sill units and some horizons are expressed simultaneously to make the better picture to understand the relative age between host rock formations and igneous intrusions. None of sill units intruded above the top of Eocene rock formation (Fig. 4.19). The youngest horizon that 4 igneous intrusions (sill unit 1-4) cross is Top Paleocene horizon (Fig. 4.19). Sill unit 5 does not cross any horizons.
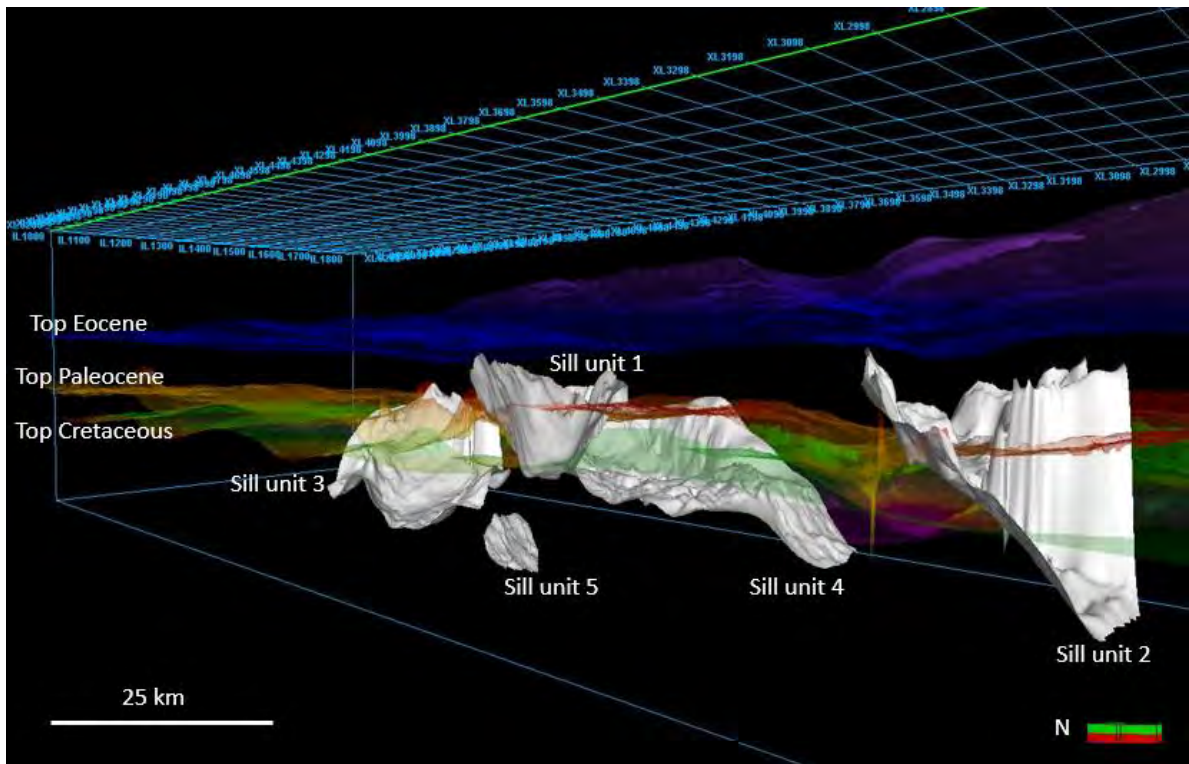
Fig. 4.19. Five sill units (White body) are showed in 3D seismic volume with horizons (translucent layer).

The summary results of each sill showing pictures and describing seismic characteristics, any measurements and geometries is given in table 1. and table 2.

TABLE 1. THE SUMMARY RESULTS OF EACH SILL (2D view).

Sill unit	2D image (Top view and profile)	Seismic characteristics	Area covering (km²) & Depth level (TWT)
1		• High amplitude • Medium to low frequency • Low continuity	• Area covering ~ 17.97 km² • The depth level: 2,450 to 3,000 ms (TWT)
2		• High amplitude • Medium frequency • Low continuity	• Area covering ~ 21.18 km² • The depth level: 2,400 to 3,200 ms (TWT)

Sill unit	2D image (Top view and profile)	Seismic characteristics	Area covering (km²) & Depth level (TWT)
3		• High amplitude • Low frequency • Medium continuity	• Area covering ~ 17.31 km² • The depth level: 3,000 to 3,300 ms (TWT)
4		• High amplitude • Low frequency • Medium continuity	• Area covering ~ 33.43 km² • The depth level: 2,900 to 3,100 ms (TWT)
5		• Medium to High amplitude • Low frequency • Low continuity	• Area covering ~ 3.81 km² • The depth level: 4,000 to 4,200 ms (TWT)

TABLE 2.THE SUMMARY RESULTS OF EACH SILL (3D view).

Sill unit	3D image of geo-body	Geometry	Dimension measurement
1	6 km / 5 km	Saucer shaped sill	Saucer shaped sill • The height is 550 ms. • The long-axis length is 3 km. • The short-axis length is 2 km.
2	Saucer shaped sill / Inclined sheet / 6.5 km / 7.5 km	Complex sill (Inclined sheeted sill + Saucer shaped sill)	Inclined sheeted sill • The height is 500 ms. • The width is 2.8 km. Saucer shaped sill • The height is 300 ms. • The long-axis length is 2.8 km. • The short-axis length is 1.7 km.
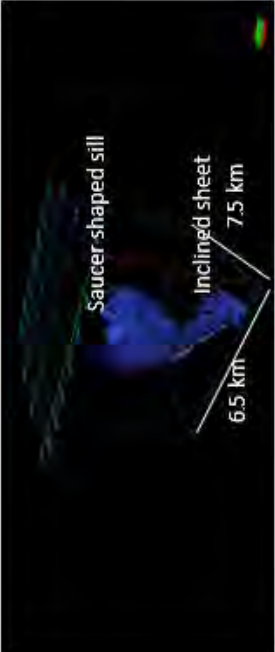
Sill unit	3D image of geo-body	Geometry	Dimension measurement
3		Inclined sheeted sill	**Inclined sheeted sill** • The height is 300 ms. • The length is 9 km.
4		Complex sill (Flattened sheeted sill + Inclined sheeted sill)	**Flattened sheeted sill** • The long axis length is 4.4 km. • The short axis length is 2.7 km. **Inclined sheeted sill** • The height is 600 ms. • The length is 6.0 km. • The width is 2.4 km.
5		Inclined sheeted sill	**Inclined sheeted sill** • The height is 200 ms. • The length is 0.75 km. • The width is 1 km.
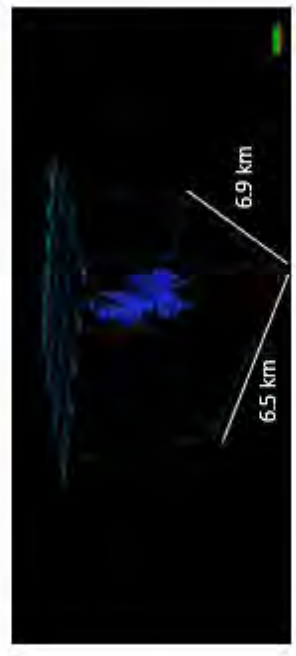
Chapter 5

Discussion

In chapter 4, the results of the study are stated, including locations, distribution, geometries and relative ages of igneous intrusions. These results will be discussed in 4 items including the effect of igneous intrusion emplacement on surroundings, relative ages of igneous intrusions, relationship to tectonic settings and magma flow.

5.1   The effects of igneous intrusion emplacement on surroundings

Igneous intrusions in the basin form by emplacement of magma intruding. During the phase of emplacement, magma intrudes the host rocks, it propagates with high temperature of heat and pressure. So, it is supposed to cause the deformation to the surroundings. The seismic reflections of surroundings above the igneous intrusion (sill unit1) are convex upward and interpreted as domal uplift or forced fold structure (Fig. 5.1). This structural feature is formed due to igneous intrusion emplacement (Polteau et al., 2008) leading to form a structural trap in petroleum systems (Kumar et al., 2013).
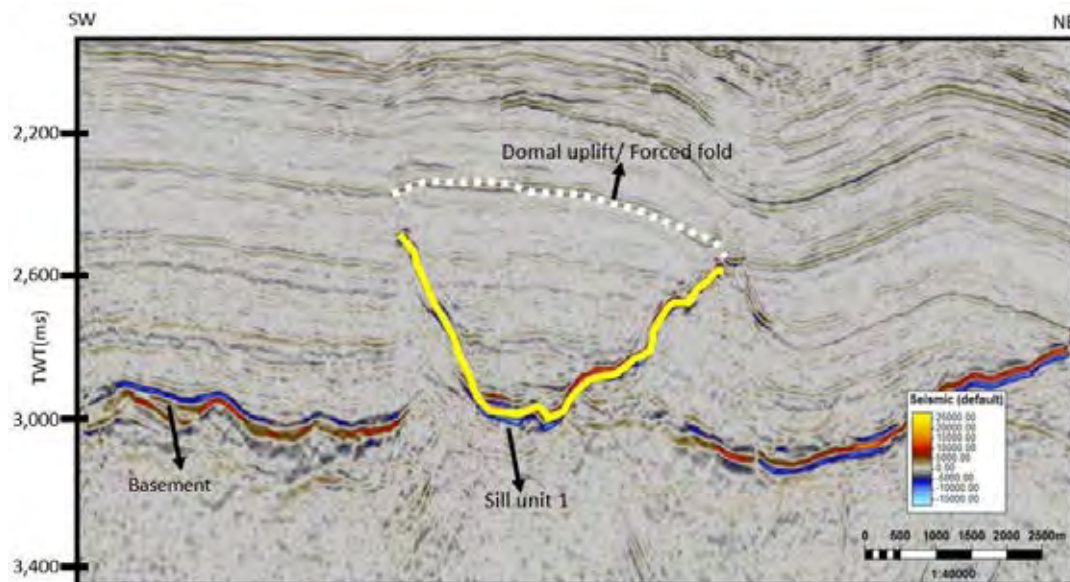
Fig. 5.1. Seismic profile showing the igneous intrusion of sill unit 1 (yellow line) and domal uplift/forced fold structure (white dot)

Interestingly, domal uplift or forced fold structure was formed above only sill unit 1 and 2 which have saucer shaped morphology while others do not; thus, the assumption is that saucer shape can induce forced fold structure (Kumar et al., 2013, Polteau et al., 2008). A simplistic kinematic model for the growth of a forced fold during the development of a saucer-shaped sill is proposed by Hansen et al. (2006) (Fig. 5.2).
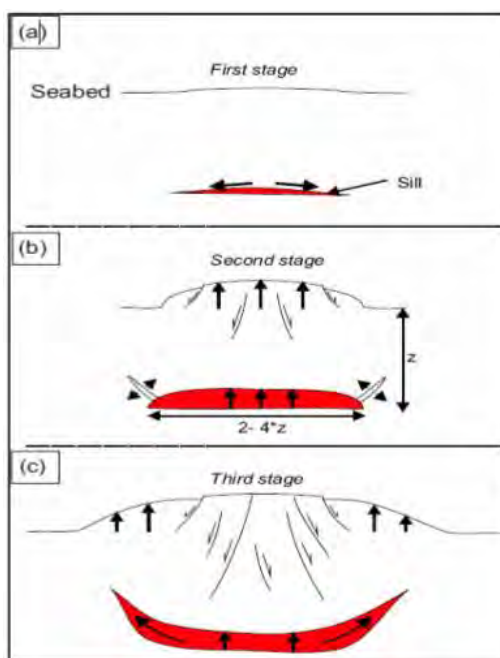
Fig. 5.2. A schematic of how forced fold structure forms derived from Hansen et al. (2006). (a) In the first stage, magma is spreading to form thin sill. (b) Spreading continues faster and causes the forced fold feature at the seabed or free surface. (c) The sill transgresses upward guided by peripheral fractures (peripheral dyke equivalent)and increased interaction with the free surface causing upward displacement along the periphery of the forced fold.

However, Revees et al. (2017) suggested that four sills in their study, S1-3 are saucer shaped sills and S4 is layer-parallel sill (comparable to sill unit 1-4 in this study respectively) induced forced fold by their interpretation. In contrast, no significant evidence of forced fold features was found above sill unit 3 (inclined sheet) and 4 (layer parallel and inclined sheet) which are not saucer shaped.

5.2   Relative ages and emplacement timing of igneous intrusions

There is no well encountering igneous intrusion in the study area. Without well data which ages or emplacement timing of igneous intrusions are difficult to be determined. However, the law of cross-cutting relationship can be applied in this situation to determine the relative ages of igneous intrusion emplacement, igneous intrusions are certainly younger than the host rocks intruded or cut by them. Sill unit 1-4 all crossed top Paleocene horizon (Fig. 4.21), the youngest horizon sills crossed, and none of these crossed top Eocene horizon (Fig. 4.20), so it can be implied that timing of emplacement of those sills is younger than Paleocene; thus, it can be interpreted that timing of sill emplacement for sill unit 1-4 is younger than Paleocene by the assumption of cross cutting relationship. Also, sill unit 5 is assumed to emplace contemporaneously with others.

Besides, some structures induced by igneous intrusion emplacement could possibly help to determine relative age or timing of emplacement; for example, forced fold caused by igneous intruding appears to be seen in limited range above igneous intrusion on a horizon that once had been the free surface when emplacement occurred (Fig. 5.2). Consequently, this characteristic is used to determine emplacement timing. The distal end of horizon affected to cause forced fold and seismic onlap onto this feature could imply the timing of emplacement which should be later than or roughly equal to the age of that horizon. Both sill units have saucer shaped morphologies inducing forced fold of the overlying rock formation till the end at the top Miocene horizon and seismic onlap is shown (Fig. 5.3a and Fig. 5.3b). As a result, emplacement timing of sill unit 1 and 2 should be younger than or roughly equal to Miocene. This corresponds to the previous assumption from cross-cutting relationship also. In short, every sill unit had emplaced simultaneously in the Canterbury since Miocene or younger.

In the other hand, Revees et al. 2017 proposed that sills emplaced principally in Oligocene, Early Miocene and Early Pliocene in their study. However, the key note is that their

sill 3 and sill 4 of their study (which are not apparently saucer shaped morphology in my view) induced forced fold in Oligocene.
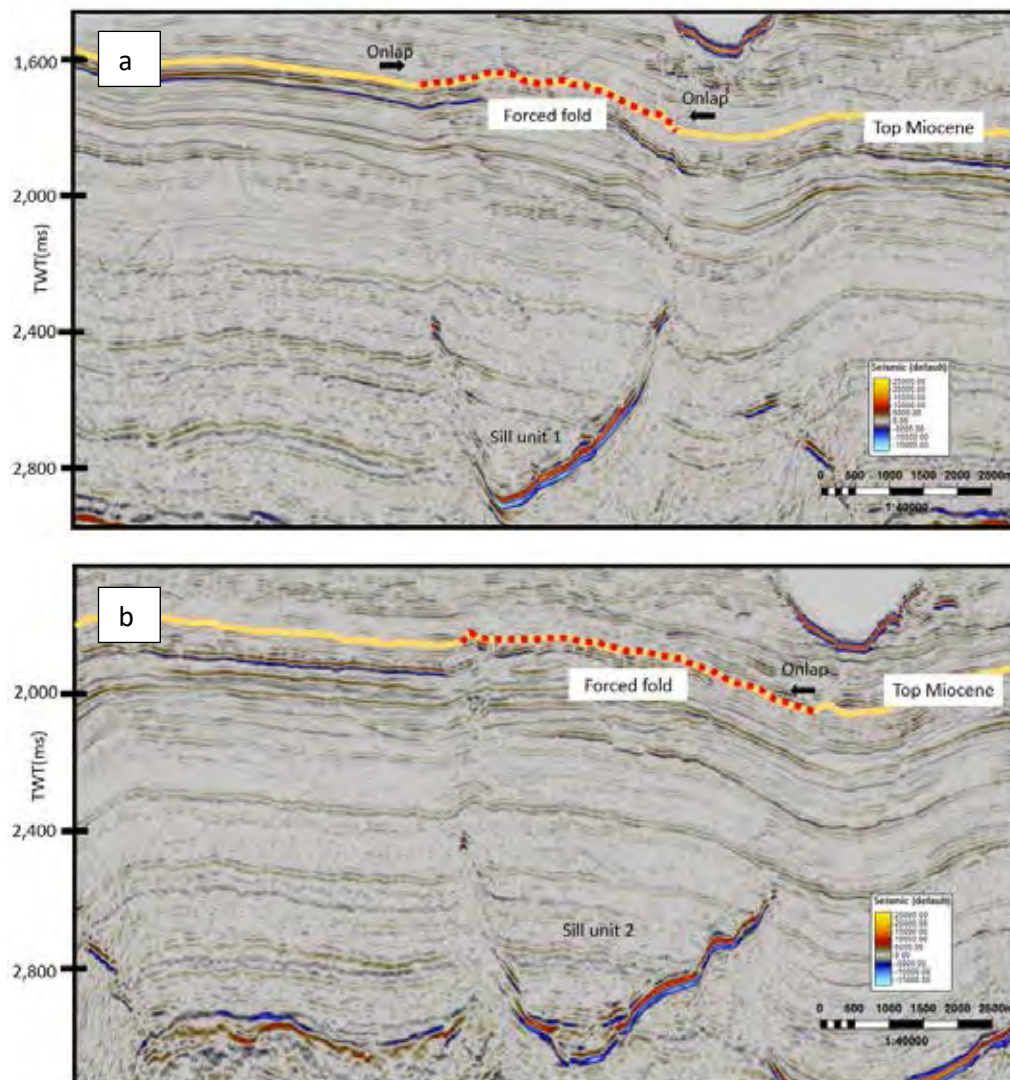
Fig. 5.3. (a) The distal end horizon of forced fold effect (Red dot) from sill unit 1 at top Miocene (Yellow line). (b) The distal end horizon of forced fold effect (Red dot) from sill unit 2 at top Miocene (Yellow line).

5.3 Relationship between igneous intrusion emplacement and tectonic settings and magmatic events in New Zealand

Sill units had occurred since Miocene, so they could possibly be influenced by tectonic settings happening from Miocene to Recent. However, there are 4 main phases of tectonic settings in the Canterbury basin stated in Chapter 2. In late Eocene, a new plate boundary propagated into New Zealand, but the Canterbury basin was outside the deformed region and continued to passively subside. Consequently, the assumption is that all units of sills were scarcely influenced by any tectonic settings occurring in the Canterbury basin. Besides, sill unit 1 and 2 have saucer shaped morphology which commonly forms in the undeformed sedimentary basin (Polteau et al, 2008), indicating that these sills was rarely affected by tectonic settings.

Additionally, all sills are assumed to emplace in the Canterbury basin during Miocene to Recent, so it can be correlated to magmatism or volcanism events in the Canterbury volcanic fields and Banks peninsular nearby the study area (Fig. 2.5). Sill emplacement could start from Miocene to Recent, so it is likely to be related to the Cookson volcanics during Miocene and View Hill, central Canterbury (Fig. 2.4). This could support the concept of several igneous events occurring intermittently and locally in New Zealand from the Late Cretaceous to the Pleistocene

5.4 Zones of magma sources and magma flow

There are 3 different morphologies of igneous intrusions in the study area, so magma flow and feeder should be also different.

5.4.1 The saucer shaped sill

The saucer-shaped sill might have dyke as a feeder at about the bottom area; however, it is rarely imaged and seen in seismic profiles (Thomson, 2007) because of survey limits like the steep dip angle. Some models propose that saucer-shaped sill intrusions form along the level of neutral buoyancy of the magma, and the feeders are expected to be

located below the outer sill at one side of the saucer (e.g., Bradley, 1965; Francis, 1982; Chevallier and Woodford, 1999), similar to this study as presented (Fig. 5.4). In contrast, other models propose that saucers are fed from below through a central feeder dyke (Malthe-Sørenssen et al., 2004; Thomson and Hutton, 2004; Galerne et al., 2008). These laccolith models controlled by discontinuities of the country rock, the feeders are expected to be located below the inner sill, resulting in radial lateral upward and outward magma flow (Fig.5.3b; e.g. Pollard and Johnson, 1973; Malthe-Sørenssen et al., 2004; Galland et al., 2008).
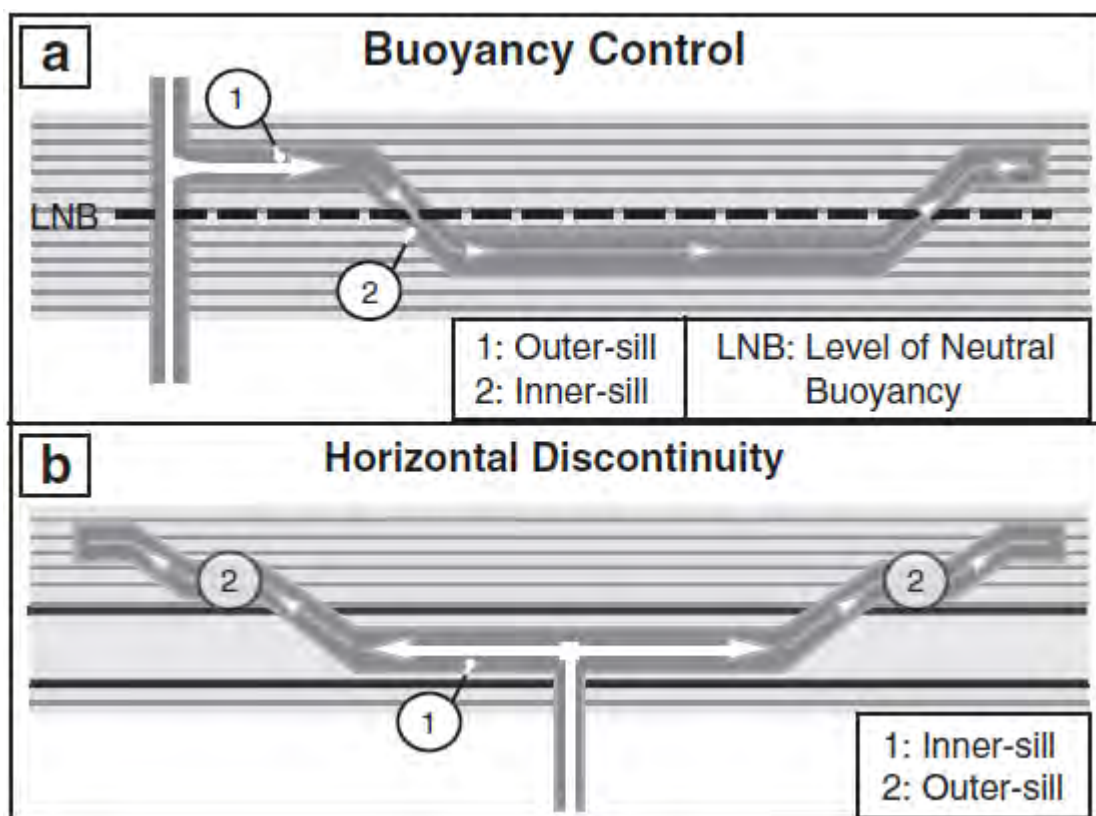
Fig. 5.4. (a) Model of emplacement controlled at the level of neutral buoyancy (LNB), Modified from Francis (Bradley, 1965; Francis, 1982 e.g. Barker, 2000). Sills are fed laterally from one part of the outer sills. (b) Model of emplacement along horizontal discontinuity (Galerne et al., 2011), derived after Malthe-Sørenssen et al. (2004).

However, in this study, sill unit 2, a sill complex, shows that inclined sheet supposed to be a dyke feeder is located underneath the inner sill of the saucer shaped sill (Fig. 5.5). Consequently, saucer shaped sills in this study is more compatible to horizontal discontinuity model.
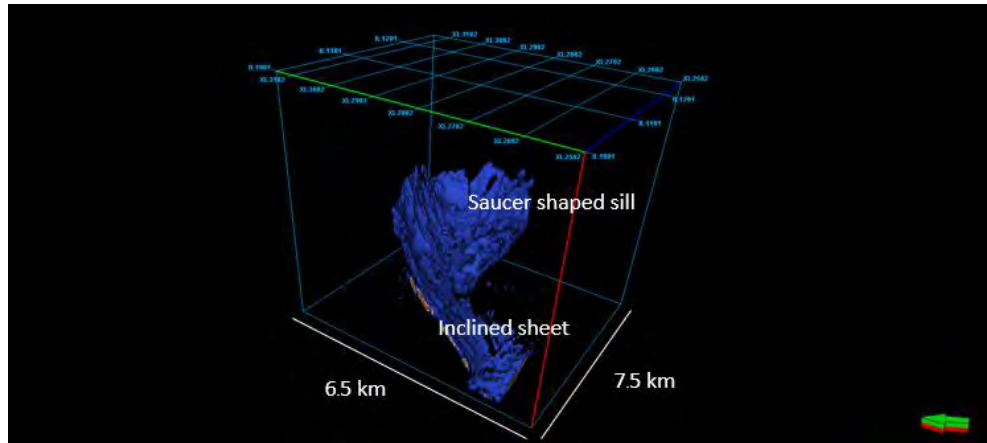
Fig. 5.5. Sill unit 2 showing that inclined sheet served as the dyke feeder to the inner sill of saucer shaped sill.

5.4.2 The inclined sheet

In most cases of sill emplacement, inclined sheets are commonly supposed to be dyke feeder (Thomson and Hutton, 2004; Magee et al., 2014) of which magma flows upward to the shallower level. The magma flow of inclined sheets is indicated by orientation of intrusive steps or bridge structure and the assumption that magma flows from the deeper level to shallower level (Naviset et al., 2017).

5.4.3 The layer-parallel sheet or concordant-strata sill

Multiple magma lobes and the styles of flow indicator can provide insights into mechanisms of layer-parallel sheet emplacement; e.g., intrusive steps, broken bridges or magma fingers (Pollard et al., 1975; Rickwood, 1990; Hutton, 2009; Schofield et al., 2012); however, based on observation, there is no such features like those appearing in any sill units in the study area.

These assumptions of flow mechanism for each morphology were applied to all sill units; thus, the magma flow pattern and potential feeder zone were derived as fallows

Sill unit 1 is saucer shaped sill that might have dyke feeder at around the center of the bottom; however, it cannot be seen in any seismic profile due to limits of survey methods. The magma flow direction is showed below (Fig. 5.6).
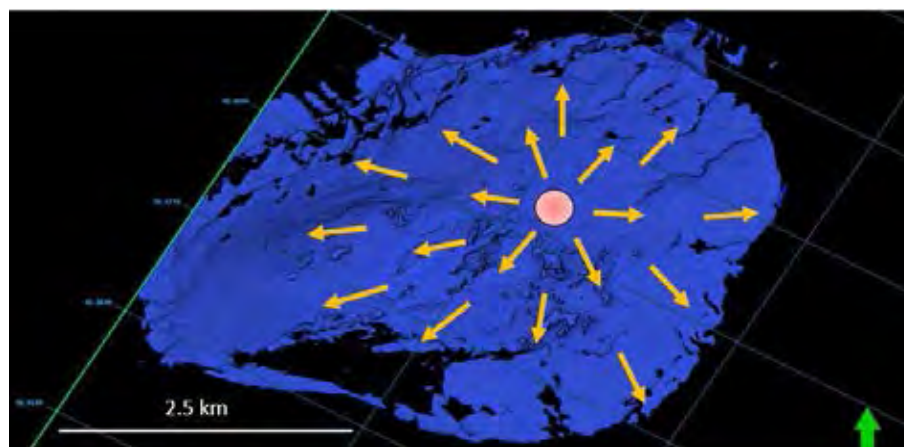
Fig. 5.6. Magma flow direction (yellow arrows) and potential feeder zone (pink circle) of sill unit 1.

Sill unit 2 is sill complex including a saucer shaped sill and an inclined sheet which is assumed to be dyke feeder of saucer shaped sill above. The magma flow direction is showed below (Fig. 5.7).
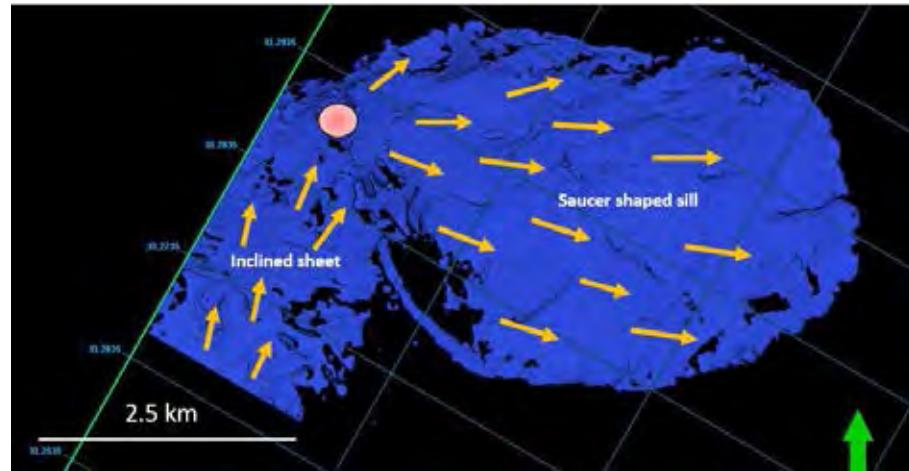
Fig. 5.7. Magma flow direction (yellow arrows) and potential feeder zone (pink circle) of sill unit 2.

Sill unit 3 is inclined sheet which has the magma flow direction showed below (Fig. 5.8).
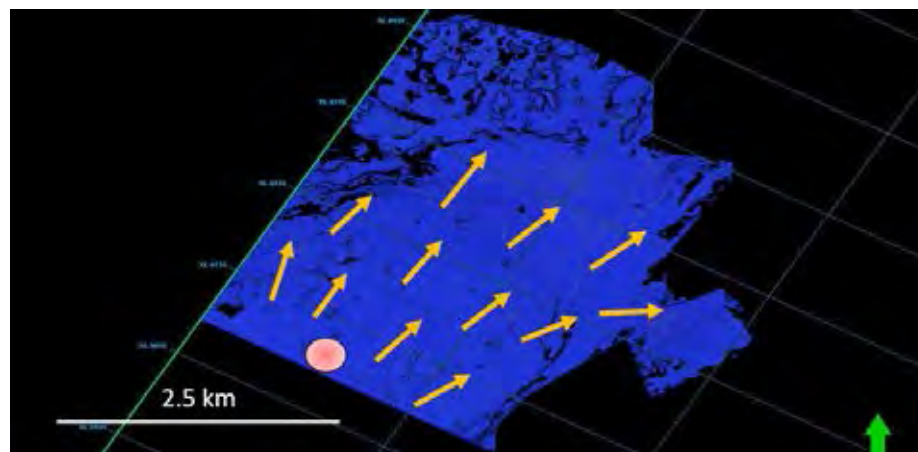
Fig. 5.8. Magma flow direction (yellow arrows) and potential feeder zone (pink circle) of sill unit 3.

Sill unit 4 is sill complex including a layer-parallel sheet and an inclined sheet. The magma flow direction is showed (Fig. 5.9). The magma flow direction of a layer parallel sheet is ambiguous; however, the assumption is that magma flow from lower to higher level (from the layer parallel sheet at lower level to the inclined sheet at higher level.)
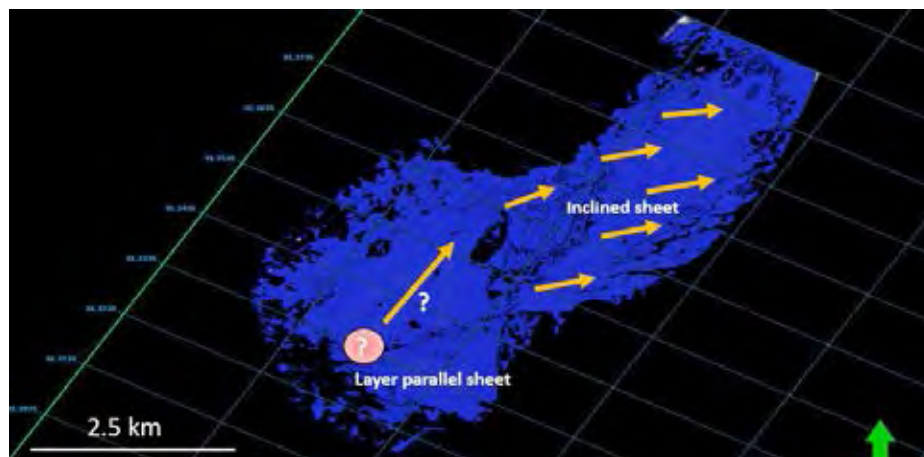
Fig. 5.9. Magma flow direction (yellow arrows) and potential feeder zone (pink circle) of sill unit 4.

Sill unit 5 is inclined sheet and patchy, so it is divided into 3 lobes which is considered as multiple magma lobes that can help constrain the potential feeder zone and magma flow pattern. The magma flow direction of sill unit 5 is showed below (Fig. 5.10).
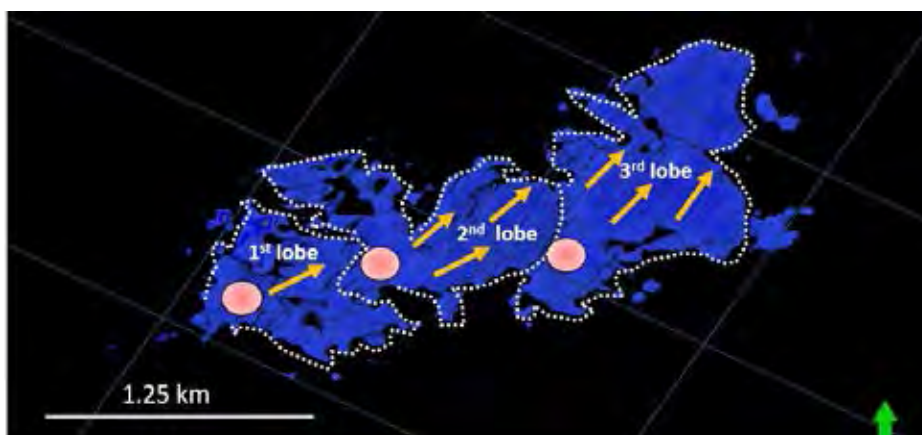
Fig. 5.10. Magma flow direction (yellow arrows) and potential feeder zone (pink circle) of sill unit 5.

5.5 Implications for hydrocarbon exploration

Igneous intrusion, having effects on host rocks and surrounding, is also important for hydrocarbon exploration because: (1) sills can induce forced folds that might potentially be structural (i.e. four-way dip closures) and stratigraphic (i.e. pinchout) traps (e.g., Reeckmann and Mebberson, 1984; Smallwood and Maresh, 2002; Schutter, 2003; Schmiedel et al., 2017), (2) intrusion-induced faulting and fracturing, which may occur with folding, can increase local permeability and porosity of reservoirs (e.g., Reeckmann and Mebberson, 1984; Holford et al., 2012), (3) The porosity can be reduced by the inelastic process (e.g., compaction and fluidization) which inhibits hydrocarbon migration and reduce reservoir quality (Schofield et al., 2017), (4) igneous intrusions can enhance thermal maturation to source rocks(Holford et al., 2013). The emplacement of sill unit 1-4 in the petroliferous Canterbury Basin since Miocene overlapped with the duration of hydrocarbon generation in the mid-Miocene (Fig. 2.5) (Bennett et al., 2000). Consequently, the force folds induced by sill unit 1 and 2 might be possible trap for hydrocarbon before its leakage at that time. All sill units except sill unit 5 intrude Cretaceous-to-Palaeogene strata, where the principal source rocks (e.g., coals) are expected (Fig. 2.4 and Fig. 4.19). However, their impact on source rock maturity is unknown due to no available well data nearby.

Chapter 6

Conclusion

In this study, 5 sill units were discovered and identified. Igneous intrusions tend to distribute mostly on the west center of the study area and cover at least 80 square kilometers approximately. Each of sills has different morphologies. Some sills are complex and have various geometries; for example, sill unit 2 has the hybridization of a saucer shaped sill and an inclined sheet, so it is called sill complex. There are 3 main morphologies found in this study including a saucer shaped, an inclined sheet, and a layer-parallel sheet morphology. All sill units had emplaced in the Canterbury basin since Miocene or younger. The saucer shaped morphology of sill unit 1 and 2 imply that these sill units were not influenced significantly by the effects of tectonic settings of the Canterbury basin. Moreover, sill unit 1 and 2, having saucer shaped morphology, induced the forced fold structure above them which could possibly be a trap for petroleum systems. The magma flow pattern is different for each morphology of sills. Radially spreading magma flow from inner to outer sills is applied to saucer shaped sill. The magma flow of inclined sheet which is commonly the dyke feeder starts from the deeper parts to the shallower ones. However, the magma flow of layer-parallel sheet in this study (sill unit 4) is still ambiguous due to lack of flow indicators like intrusive steps, broken bridge structure and magma fingers.

References

Barker, D.S., 2000. Emplacement of a xenolith-rich sill, Lajitas, Texas. Journal of Volcanology and Geothermal Research 104, 153–168.

Bradley, J., 1965, Intrusion of major dolerite sills. Transactions of the Royal Society of New Zealand 3, 27-55.

Bennett, D., Brand, R., Francis, D., Langdale, S., Mills, C., Morris, B., & Tian, X., 2000. Preliminary results of exploration in the onshore Canterbury Basin. Paper presented at the 2000 New Zealand Petroleum Exploration Conference Proceedings.

Carter, R., 1988, Post-breakup stratigraphy of the Kaikoura 5 Synthem (Cretaceous-Cenozoic), continental margin, southeastern New Zealand. New Zealand journal of geology and geophysics, 31(4), 405-429. http://dx.doi.org/10.1080/00288306.1988.10422141

Chevallier, L., & Woodford, A., 1999, Morpho-tectonics and mechanism of emplacement of the dolerite rings and sills of the western Karoo, South Africa. South African Journal of Geology 102 (1), 43–54.

Clouard, V., & Bonneville, A., 2005. Ages of seamounts, islands and plateaus and plateaus on the Pacific plate. In: Foulger, G.R., Natland, J.H., Presnall, D.C., Anderson, D.L. (Eds.), Plates, Plumes, and Paradigms. Geological Society of America Special Paper: Geological Society of America, vol. 388, 71–90.

Constable, R., & R. Crookbain, 2011, A sequence stratigraphic study of the Great South Basin: New Zealand open-file Petroleum Report 4348. Wellington, Ministry of Economic Development.

Cook, C., Briggs, R.M., Smith, I.E.M., & Maas, R., 2004, Petrology and geochemistry of intraplate basalts in the South Auckland Volcanic Field, New Zealand: evidence for two coeval magma suites from distinct sources. Journal of Petrology 46, 473–503.

Cox, S., & Sutherland, R., 2007. Regional Geological Framework of South Island, New Zealand, and its Significance for Understanding the Active Plate Boundary. Washington DC American Geophysical Union Geophysical Monograph Series. 175. 19-46. 10.1029/175GM03.:

Field, B.D., & G.H. Browne, 1989, Cretaceous and Cenozoic sedimentary basins and geological evolution of the Canterbury region, South Island, New Zealand: New Zealand Geological Survey Basin Studies 2, Wellington, Institute of Geological & Nuclear Sciences.

Fjeldskaar, W., H. M. Helset, H. Johansen, I. Grunnaleite, & I. Horstad, 2008, Thermal modeling of magmatic intrusions in the Gjallar Ridge, Norwegian Sea: Implications for vitrinite reflectance and hydrocarbon maturation, Basin Res., 20, 143–159.

Francis, E.H., 1982, Magma and sediment—I. Emplacement mechanism of late Carboniferous tholeiite sills in northern Britain. Journal of the Geological Society, London 139 (1), 1–20.

Fulthorpe, C. S., Carter, R. M., Miller, K. G., & Wilson, J., 1996, Marshall Paraconformity: a mid-Oligocene record of inception of the Antarctic circumpolar current and coeval glacio-eustatic lowstand? Marine and petroleum geology, 13(1), 61-77. https://doi.org/10.1016/0264-8172(95)00033-X

Galerne, C.Y., Neumann, E.R., & Planke, S., 2008, Emplacement mechanisms of sill complexes: information from the geochemical architecture of the Golden Valley Sill Complex, South Africa. Journal of Volcanology and Geothermal Research 177 (2), 425–440.

Galerne, C.Y., Galland, O., Neumann, E.R., & Planke, S., 2011, 3D relationships between sills and their feeders: Evidence from the Golden Valley Sill Complex (Karroo Basin) and experimental modeling: Journal of Volcanology and Geothermal Research, v. 202, 189–199, doi:10.1016/j.jvolgeores.2011.02.006.

Galland, O., Planke, S., Neumann, E.R., & Malthe-Sørenssen, A., 2009, Experimental modelling of shallow magma emplacement: application to saucer-shaped intrusions. Earth and Planetary Science Letters 277 (3–4), 373–383.

Galushkin, Y. I., 1997, Thermal effects of igneous intrusions on maturity of organic matter: A possible mechanism of intrusion, Org. Geochem., 26(11–12), 645–658.

Ghisetti, F. C., & Sibson, R. H., 2012, Compressional reactivation of E–W inherited normal faults in the area of the 2010–2011 Canterbury earthquake sequence. New Zealand Journal of Geology and Geophysics, 55(3), 177-184. https://doi.org/10.1785/gssrl.82.6.824

Griffin, A.G., 2013, Petroleum well summary sheets from selected frontier basins, New Zealand: Canterbury, Great South and Northland basins: Wellington, Institute of Geological & Nuclear Sciences.

Hansen D.M. & Joseph Cartwright, 2006, Magma transport through the crust via interconnected sill complexes, Geological Society of America, v. 34; no. 11; 929-932.

Holford, S. P., Schofield, N., MacDonald, J. D., Duddy, I. R., & Green, P. F., 2012, Seismic analysis of igneous systems in sedimentary basins and their impacts on hydrocarbon prospectivity: 5 examples from the southern Australian margin. APPEA Journal, 52, 23. https://doi.org/10.1071/AJ11017

Holford, S. P., Schofield, N., Jackson, C. A. L., Magee, C., Green, P. F., & Duddy, I. R. 2013, Impacts of igneous intrusions on source and reservoir potential in prospective sedimentary basins along the western Australian continental margin. In M. Keep & S. J. Moss (Eds.), The Sedimentary Basins of Western Australia IV. Perth, WA: Proceedings of the 10 Petroleum Exploration Society of Australia Symposium.

Hoernle, K., White, J.D.L., Bogaard, P.V.D., Hauff, F., Coombs, D.S., Werner, R., Timm, C., Garbe-Schönberg, C.-D., Reay, A., & Cooper, A.F., 2006, Cenozoic intraplate volcanism on New Zealand: upwelling induced by lithospheric removal. Earth and Planetary Science Letters 248, 335–352.

Hutton, D.H.W., 2009, Insights into magmatism in volcanic margins: Bridge structures and a new mechanism of basic sill emplacement—Theron Mountains, Antarctica: Petroleum Geoscience, v. 15, 269–278, doi: 10 .1144 /1354 -079309 -841.

Killops, S., Cook, R., Sykes, R., & Boudou, J. 1997, Petroleum potential and oil source correlation in the Great South and Canterbury Basins. New Zealand journal of geology and geophysics, 40(4), 405-423. 25 http://dx.doi.org/10.1080/00288306.1997.9514773

Kumar, J., Negi, M.S., Singh, P., & Sharma, R., 2013, Identification of forced folds or jacked up structures in Satpura Basin: An attractive hydrocarbon play, in Kochi, 2013: 10th Biennial International Conference and Exposition, 129–135.

Lu, H., Fulthorpe, C. S., Mann, P., & Kominz, M. A., 2005, Miocene–Recent tectonic and climatic controls on sediment 30 supply and sequence stratigraphy: Canterbury basin, New Zealand. Basin Research, 17(2), 311-328. http://dx.doi.org/10.1111/j.1365-2117.2005.00266.x

Magee, C., McDermott, K.G., Stevenson, C.T., & Jackson, C.A.-L., 2014, Influence of crystallized igneous intrusions on fault nucleation and reactivation during continental extension: Journal of Structural Geology, v. 62, 183–193, doi:10.1016/j.jsg.2014.02.003.

Malthe-Sørenssen, A., Planke, S., Svensen, H., & Jamtveit, B., 2004, Formation of saucer shaped sills. In: Breitkreuz, C., Petford, N. (Eds.), Physical Geology of High-Level Magmatic Systems: Geological Society, London, Special Publication, 215–227.

Millett, J.M., Wilkins, A.D., Campbell E., Hole, M.J., Taylor, R.A., Healy, D., Jerram, D.A., Jolley, D.W., Planke, S., Archer, S.G., & Blischke, A., 2016, The geology of offshore drilling through basalt sequences: Understanding operational complications to improve efficiency: Marine and Petroleum Geology, v. 77, 1177–1192, doi:10.1016/j.marpetgeo.2016.08.010.

Naviset, S., Morley C.K., Naghadeh D.H., & Ghosh J., 2017, Sill emplacement during and inversion from three-dimensional seismic and well data, Phitsanulok basin, Thailand. Geosphere, v. 13, no. 6, 1-24 doi:10.1130/GES01466.1. doi:10.1130/GES01466.1.

Pollard, D.D., & Johnson, A.M., 1973, Mechanics of growth of some laccolithic intrusions in the Henry Mountains, Utah. II. Bending and failure of overburden layers and sill formation. Tectonophysics 18, 311–354.

Pollard, D.D., Muller, O.H., & Dockstader, D.R., 1975, The form and growth of fingered sheet intrusions: Geological Society of America Bulletin, v. 86, 351–363, doi: 10 .1130 /0016 -7606 (1975)86 <351: TFAGOF>2 .0 .CO;2.

Polteau, S., Mazzini, A., Galland, O., Planke, S., & Malthe-Sørenssen, A., 2008, Saucer shaped intrusions: Occurrences, emplacement and implications: Earth and Planetary Science Letters, v. 266, 195–204, doi:10.1016/j.epsl.2007.11.015.

Reeckmann, S. A., & Mebberson, A. J., 1984, Igneous intrusions in the North-West Canning Basin and their impact on oil exploration. In P. G. Purcell (Ed.), The Canning Basin, WA (pp. 389-399). Perth, WA: Proceedings of the Geological Society of Australia/Petroleum Exploration Society of Australia Canning Basin Symposium.

Reeves, J., Magee, C., & Jackson, C. A., 2017. Unravelling intrusion-induced forced fold kinematics and ground deformation using 3D seismic reflection data. Retrieved from eartharxiv.org/na62q

Rickwood, P., 1990, The anatomy of a dyke and the determination of propagation and magma flow directions, in Parker, A.J., et al., eds., Mafic dykes and emplacement mechanisms: Rotterdam, Balkema, 81–100.

Sahoo, R.T., Kroeger, K.F., Thrasher, G., Munday, S., Mingard, H., Cozens, N., & Hill, M. 2015, Facies distribution and impact on petroleum migration in the Canterbury basin, New Zealand: Search and Discovery Article, 1-19

Schmiedel, T., Kjoberg, S., Planke, S., Magee, C., Galland, O., Schofield, N., & Jerram, D. A., 2017, Mechanisms of overburden deformation associated with the emplacement of the Tulipan sill, mid-Norwegian margin. Interpretation, 5(3), SK23-SK38. https://doi.org/10.1190/INT-2016-0155.1

Schofield, N., Heaton, L., Holford, S.P., Archer, S.G., Jackson, A-L.C., & Jolley, D.W. 2012, Seismic imaging of 'broken bridges': liking seismic to outcrop-scale investigations of intrusive magma lobes: Journal of the Geological Society, v.169; 421-426.

Schofield, N., Holford, S., Millett, J., Brown, D., Jolley, D., Passey, S. R., . . . Stevenson, C., 2017. Regional magma plumbing and emplacement mechanisms of the Faroe-Shetland Sill Complex:

implications for magma transport and petroleum systems within sedimentary basins. Basin Research, 29(1), 41-63. https://doi.org/10.1111/bre.12164

Schutter, S. R., 2003, Hydrocarbon occurrence and exploration in and around igneous rocks. Geological Society, London, Special Publications, 5 214(1), 7-33. https://doi.org/10.1144/GSL.SP.2003.214.01.02

Shell BP Todd, 1984, Interpretation and prospectivity of PPL 38203 Canterbury Basin New Zealand: Ministry of Economic Development, Wellington, unpublished open-file Petroleum Report 1046.

Smallwood, J.R., & Maresh, J. 2002, The properties, morphology and distribution of igneous sills: modelling, borehole data and 3D seismic data from the Faeroe–Shetland area. In: Jolley, D.W. & Bell, B.R. (eds) The North Atlantic Igneous Province: Stratigraphy, Tectonic, Volcanic and Magmatic Processes. Geological Society, London, Special Publications, 197, 271–306.

Smith, I.E.M., Okada, T., Itaya, T., & Black, P.M., 1993, Age relationships and tectonic implications of late Cenozoic basaltic volcanism in Northland, New Zealand. New Zealand Journal of Geology and Geophysics 36, 385–393.

Sutherland, R., & Browne, G., 2003, Canterbury basin offers potential on South Island, New Zealand: Oil and Gas Journal, 45-49.

Sykes, R., & Funnell, R.H., 2002, Petroleum source rock potential and generation history in the offshore Canterbury Basin: New Zealand open-file Petroleum Report 2707. Wellington, Ministry of Economic Development.

Thomson, k. & Hutton, D., 2004, Geometry and growth of sill complexes: insights using 3D seismic from the North Rockall Trough. Bulletin of Volcanology, 66, 364–375.

Thomson, K., 2007, Determining magma flow in sills, dykes and laccoliths and their implications for sill emplacement mechanisms. Bulletin of Volcanology 70 (2), 183–201.

Timm, C., Hoernle, K., Bogaard, P.V.D., Bindemann, I., & Weaver, S.D., 2009, Geochemical evolution of intraplate volcanism at Banks Peninsula, New Zealand: interaction between asthenospheric and lithosphericmelts. Journal of Petrology 50 (6), 989–1023.

Timm, C., Hoernle, K., Werner, R., Hauff, F., van den Bogaard, P., White, J., . . . Garbe-Schönberg, D., 2010, Temporal and 20 geochemical evolution of the Cenozoic intraplate volcanism of Zealandia. Earth-Science Reviews, 98(1), 38-64. https://doi.org/10.1016/j.earscirev.2009.10.002

Uruski, C. I., 2010, New Zealand's deepwater frontier. Marine and petroleum geology, 27(9), 2005-2026. 25 https://doi.org/10.1016/j.marpetgeo.2010.05.010